Membrane recruitment of the cargo-selective retromer subcomplex is catalysed by the small GTPase Rab7 and inhibited by the Rab-GAP TBC1D5

Matthew N. J. Seaman*, Michael E. Harbour, Daniel Tattersall‡, Eliot Read§ and Nicholas Bright

University of Cambridge, Cambridge Institute for Medical Research, Department of Clinical Biochemistry, Wellcome Trust/MRC Building, Addenbrookes Hospital, Hills Road, Cambridge CB2 0XY, UK

*Author for correspondence (e-mail: mnjs100@cam.ac.uk)

‡Present address: Centre for Cutaneous Research, Institute of Cell and Molecular Science, 4 Newark Street, Whitechapel, London E1 2AT, UK

§Present address: University of Cambridge, Department of Pathology, Tennis Court Road, Cambridge CB2 1QP, UK

Accepted 24 March 2009
Journal of Cell Science 122, 2371-2382 Published by The Company of Biologists 2009
doi:10.1242/jcs.048686

Summary

Retromer is a membrane-associated heteropentameric coat complex that functions in the endosome-to-Golgi retrieval of the cation-independent mannose-6-phosphate receptor, the Wntless protein and other membrane proteins of physiological significance. Retromer comprises two functional subcomplexes: the cargo-selective subcomplex is a trimer of the VPS35, VPS29, VPS26 proteins, whereas the sorting nexin proteins, Snx1 and Snx2 function to tubulate the endosomal membrane. Unlike the sorting nexins, which contain PtdIns3*P*-binding PX domains, the cargo-selective VPS35/29/26 complex has no lipid-binding domains and its recruitment to the endosomal membrane remains mechanistically uncharacterised. In this study we show that the VPS35/29/26 complex interacts with the small GTPase Rab7 and requires Rab7 for its recruitment to the endosome. We show that the Rab7K157N mutant that causes the peripheral neuropathy, Charcot-Marie-Tooth disease, does not interact with the VPS35/29/26 complex, resulting in a weakened association with the membrane. We have also identified a novel retromer-interacting protein, TBC1D5, which is a member of the Rab GAP family of proteins that negatively regulates VPS35/29/26 recruitment and causes Rab7 to dissociate from the membrane. We therefore propose that recruitment of the cargo-selective VPS35/29/26 complex is catalysed by Rab7 and inhibited by the Rab-GAP protein, TBC1D5.

Supplementary material available online at
http://jcs.biologists.org/cgi/content/full/122/14/2371/DC1

Key words: Endosome, Rab-GAP, Rab7, Recruitment, Retromer

Introduction

The steady-state localisation of membrane proteins within the secretory and endocytic pathways is the result of dynamic sorting mechanisms in which membrane-associated coat proteins recognise distinct motifs within the cytoplasmic tails of membrane proteins to direct the membrane protein into a specific pathway (reviewed by Mancias and Goldberg, 2005; Béthune et al., 2006; Seaman, 2008). The coatomer/COPI coat recognises di-lysine motifs comprising KKxx or KxKxx to sort membrane proteins into a Golgi-to-endoplasmic reticulum (ER) pathway (Letourneur et al., 1994). Clathrin with the AP-1 adaptor binds to YxxΦ motifs at the *trans*-Golgi network (TGN) to sort membrane proteins into clathrin-coated vesicles (CCVs) (Bonifacino and Traub, 2003).

Before the cytoplasmic coat can recognise and sort cargo proteins, the coat complex must be recruited to the appropriate membrane. This key regulatory step is often mediated by small guanine triphosphate (GTP) hydrolases (GTPases) that regulate coat recruitment through the binding and hydrolysis of GTP (reviewed by Spang, 2008). Both coatomer/COPI and AP-1 are recruited to Golgi or TGN membranes by the small GTPase ADP-ribosylation factor-1 (ARF1) (Stamnes and Rothman, 1993; Palmer et al., 1993; Orci et al., 1993). Interestingly, COPI also interacts with an ARF1 GTPase activating protein (GAP) that promotes the hydrolysis of GTP by ARF1, thereby triggering the release of ARF1 and coatomer/COPI from the membrane (Eugster et al., 2000; Szafer et al., 2001). Through its interactions with ARF1 and the ARF1 GAP, coatomer/COP-1 thereby regulates its own membrane association. The ARF1-related small GTPase, Sar1, functions in both yeast and mammalian cells to drive recruitment of the COPII coat to the ER and the Sec23 component of the COPII coat complex acts as a GAP for Sar1 producing a similar self-regulatory loop to that for ARF1 and coatomer/COPI (Yoshihisa et al., 1993; Barlowe et al., 1994).

The Rab family of small GTPases also have a crucial regulatory role in the secretory and endocytic pathways by functioning as organisers of discrete regions of the endo-membrane system and by mediating the tethering interactions that precede docking and fusion of donor and acceptor membranes (reviewed by Fukuda, 2008; Zerial and McBride, 2001). Amongst the best characterised of the Rab proteins are Rab5 and Rab7. The Rab5 protein acts early in the endocytic pathway and is required for the fusion of endocytic vesicles and early endosomes (Bucci et al., 1992). Rab5 has also been shown to regulate the dynamics of CCVs at the plasma membrane (McLauchlan et al., 1998; Semerdjieva et al., 2008). Rab7 acts later in the endocytic pathway and is required to mediate the fusion of late-endosomes with lysosomes (Bucci et al., 2000). As early endosomes mature they undergo 'Rab conversion' in which Rab5 is progressively displaced by Rab7 (Rink et al., 2005). This process occurs simultaneously with the dynein-mediated movement of endosomes down microtubules from the periphery of the cell towards the microtubule-organising centre in the perinuclear region (Johansson et al., 2007; Driskell et al., 2007).

The retromer complex is a cytoplasmic coat complex in the endosome-to-Golgi retrieval pathway (Seaman, 2004; Arighi et al., 2004) that recognises hydrophobic motifs to sort proteins such as the cation-independent mannose-6-phosphate receptor (CI-MPR) and sortilin for retrieval to the Golgi (Seaman, 2007). Retromer also mediates the trafficking of the Wntless protein, which is crucial for secretion of the morphogen Wnt (Eaton, 2008). Retromer has also been implicated in regulating the localisation and processing of amyloid precursor protein (APP), establishing it as a key player in the pathogenesis of Alzheimer's disease (Small et al., 2005; Muhammad et al., 2008).

Retromer is a heteropentamer that comprises two distinct subcomplexes (reviewed by Seaman, 2005). The VPS35/29/26 complex forms a stable trimer that selects cargo for endosome-to-Golgi retrieval (Collins et al., 2008; Nothwehr et al., 2000). The other components of retromer, Snx1 and Snx2 in mammals and Vps5p and Vps17p in yeast are members of the sorting nexin family of proteins and bind to endosomal membranes through conserved p40 Phox homology (PX) domains that recognise phosphotidylinositol 3-phosphate (PtdIns3*P*) (Haft et al., 2000; Carlton et al., 2004; Rojas et al., 2007; Burda et al., 2002). The sorting nexin components of retromer are believed to have a more structural role by tubulating the endosomal membrane through the Bin-amphiphysin-Rvs (BAR) domains present in their respective C-termini (Cullen, 2008). A critical aspect to retromer function that remains to be fully understood is the recruitment of the cargo-selective VPS35/29/26 complex to the endosomal membrane, a process that will have a vital regulatory role in the interaction(s) between VPS35/29/26 and cargo proteins such as the CI-MPR and Wntless. Unlike the sorting nexins, the VPS35/29/26 complex does not possess any lipid binding domain(s) to mediate its recruitment which gives rise to the question: how is the cargo-selective VPS35/29/26 complex targeted and recruited to the endosomal membrane?

In this study, we have investigated the interaction between the cargo-selective VPS35/29/26 subcomplex and the small GTPase Rab7, and we report that the VPS35/29/26 complex is recruited to endosomal membranes in a Rab7-dependent manner. Loss of Rab7 expression results in the VPS35/29/26 complex redistributing to the cytoplasm and results in a defect in endosome-to-Golgi retrieval. The VPS35/29/26 complex fails to interact with a Rab7 mutant (K157N) that causes the neurodegenerative disorder, Charcot-Marie-Tooth disease (type 2B) and is weakly membrane associated when the only Rab7 protein present is the K157N mutant. We additionally report that retromer interacts with an uncharacterised Rab-GAP, TBC1D5, which negatively regulates retromer recruitment and causes Rab7 to redistribute to the cytoplasm.

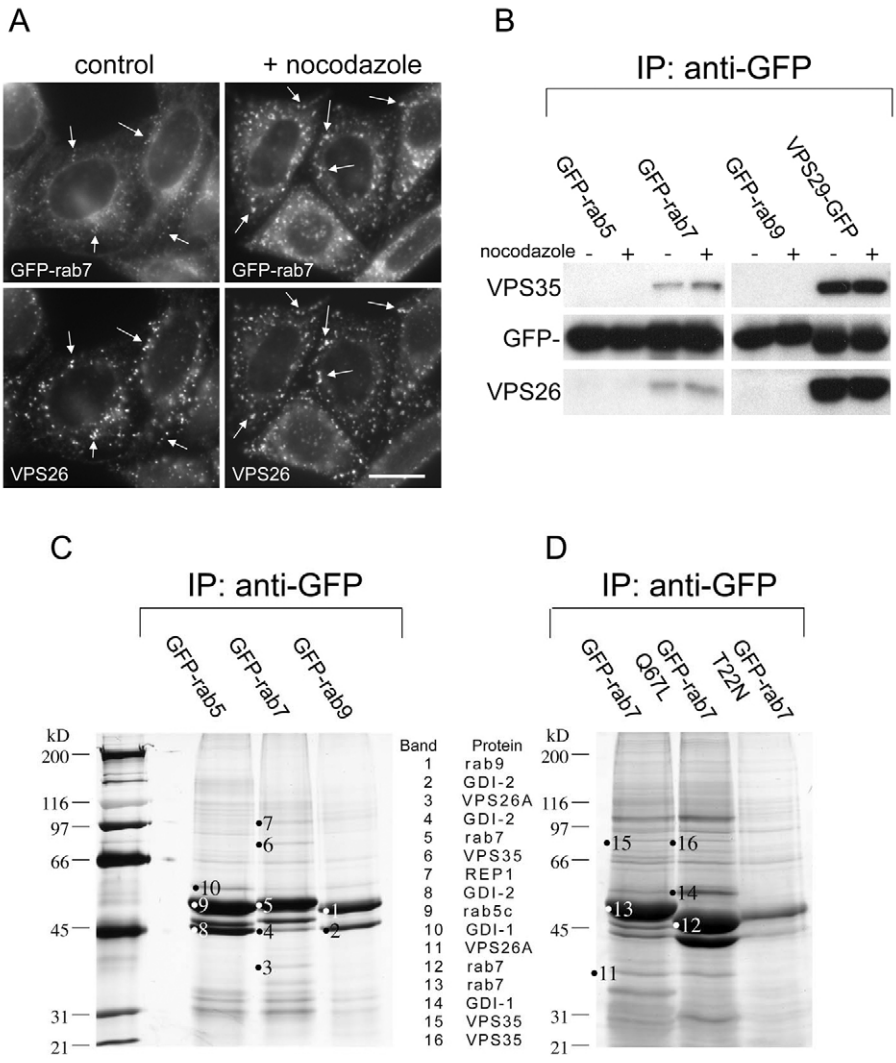

Fig. 1. VPS35/29/26 interacts with Rab7. (A) Cells stably expressing GFP-Rab7 were treated with nocodazole before fixation and labelling with antisera against VPS26. There is some colocalisation between VPS35/29/26 and GFP-Rab7 (indicated by arrows), which is enhanced by treatment with nocodazole. Scale bar: 20 µm. (B) Cells expressing GFP-tagged Rab5, Rab7, Rab9 or VPS29 were treated with nocodazole, lysed and then incubated with anti-GFP. After washing, the immunoprecipitated proteins were subjected to SDS-PAGE and western blotting with anti-VPS35 and anti-VPS26. VPS35/29/26 interacts substoichiometrically with GFP-Rab7 but not GFP-Rab5 or GFP-Rab9. (C) Cells expressing GFP-Rab5, GFP-Rab7 or GFP-Rab9 were treated with nocodazole, lysed and incubated with anti-GFP. The immunoprecipitated proteins were analysed by SDS-PAGE, silver staining and mass spectrometry. VPS35 and VPS26 were detected in the Rab7 lane along with Rab escort protein and GDI-2. (D) Cells expressing GFP-Rab7, GFP-Rab7Q67L or GFPRab7T22N were treated as above except that there was no incubation with nocodazole before lysis and immunoprecipitation with anti-GFP. VPS35 and VPS26 were detected in the GFP-Rab7 and GFP-Rab7Q67L lanes.

Recruitment of the cargo-selective retromer subcomplex to the endosome membrane is therefore regulated by the small GTPase Rab7 and a Rab-GAP protein in a manner similar to other vesicle coats such as COPII and coatomer/COPI.

Results

The VPS35/29/26 complex interacts with Rab7

In our previous studies we have shown that retromer colocalises with both Rab5 and Rab7 (Seaman, 2004) and there is compelling evidence from studies by Pfeffer and colleagues that Rab9 is required for endosome-to-Golgi retrieval of the CI-MPR (Riederer et al., 1994; Reddy et al., 2006). Data from the amoeba, *Entamoeba hystolytica* have shown that the amoebic equivalent of Rab7 can interact with amoebic VPS35/29/26 (Nakada-Tsukui et al., 2005). Therefore, in initial experiments, cells stably expressing GFP-Rab7 were analysed for colocalisation with retromer. There was colocalisation between VPS26 and GFP-Rab7, which was enhanced after treatment with the microtubule-depolymerising drug nocodazole (Fig. 1A). To determine whether retromer interacts with Rab7, native immunoprecipitations were performed on cells stably expressing GFP-Rab5, GFP-Rab7, GFP-Rab9 or VPS29-GFP in the presence or absence of nocodazole. VPS35 and VPS26 co-immunoprecipitated with GFP-Rab7 but not with GFP-Rab5 or GFP-Rab9 (Fig. 1B). VPS35 and VPS26 form a high-affinity complex with VPS29, with a stoichiometry of 1:1:1 (Collins et al., 2005; Hierro et al., 2007; Collins et al., 2008) and therefore VPS29-GFP serves as a positive control in this experiment. VPS35 and VPS26 strongly co-immunoprecipitated with VPS29-GFP whereas the interaction with GFP-Rab7 was substoichiometric.

The interaction between Rab7 and retromer was further investigated by scaling up the number of cells used and then analysing the results by SDS-PAGE. In Fig. 1C, four 140 mm dishes of cells expressing either GFP-Rab5, GFP-Rab7 or GFP-Rab9 were treated with nocodazole before lysis and incubation with anti-GFP covalently coupled to Sepharose. The bound proteins were eluted at low pH, precipitated and then subjected to SDS-PAGE followed by silver staining. VPS35 and VPS26 were detected by mass spectrometry (for details see supplementary material Table S1) in the sample from GFP-Rab7 cells, but were absent in the samples from GFP-Rab5 and GFP-Rab9 cells. Other proteins detected included Rab guanine dissociation inhibitor 1 (GDI1) and GDI2 and Rab escort protein-1 (REP1). Single point mutations in Rab proteins can be used to 'lock' the protein in an active GTP-bound, or inactive GDP-bound state. In another native immunoprecipitation experiment, cells stably expressing either GFP-Rab7, GFP-Rab7Q67L (GTP-locked) or GFP-Rab7T22N (GDP-locked) were lysed and incubated with anti-GFP coupled to Sepharose. The precipitated proteins were analysed by SDS-PAGE and mass spectrometry (Fig. 1D; supplementary material Table S1). VPS35 and VPS26 were detected in samples from GFP-Rab7 and GFP-Rab7Q67L cells but not GFP-Rab7T22N cells although the GFP-Rab7T22N mutant was poorly expressed relative to GFP-Rab7 and GFP-Rab7Q67L.

From the native immunoprecipitation data in Fig. 1C,D it is apparent that VPS35/29/26 can interact with both GFP-Rab7 and the GTP-locked Q67L mutant. To determine where these interactions occur, cells expressing GFP-Rab7 or GFP-Rab7Q67L were examined using the higher resolving power of electron microscopy (EM). In our previous studies we have used a quick freeze-thaw technique to permeabilise cells, which are then accessible to antibody labelling before embedding in resin (Seaman, 2004). Therefore, cells expressing GFP-Rab7 or GFP-Rab7Q67L were snap frozen, thawed, fixed and then labelled with antibodies against VPS26 and GFP followed by 5 nm and 10 nm colloidal gold labelled secondary antibodies before embedding in resin and sectioning for EM. Cells expressing GFP-Rab7 are shown in Fig. 2A-C, whereas GFP-Rab7Q67L cells are shown in Fig. 2D-F. To more easily distinguish the two sizes of colloidal gold particles, the 5 nm and 10 nm gold particles have been false coloured. Unaltered versions of the micrographs are in supplementary material Fig. S1. In cells expressing both GFP-Rab7 and GFP-Rab7Q67L, there was significant colocalisation of VPS26 (5 nm gold particles, coloured blue) and GFP (10 nm gold particles, coloured yellow).

GDP-locked Rab7 inhibits VPS26 recruitment

If the VPS35/29/26 complex is able to interact with the wild type and GTP-locked Q67L mutant then what happens to the VPS35/29/26 complex in cells expressing the GDP-locked T22N mutant? This question was addressed firstly by investigating the localisation of VPS26 in cells stably expressing GFP-Rab7T22N. In Fig. 3A, cells expressing GFP-Rab7T22N were mixed with

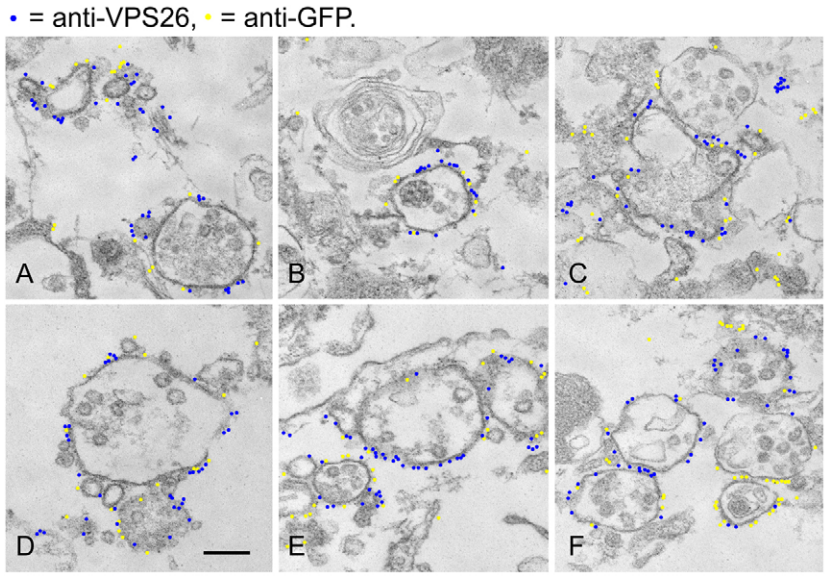

Fig. 2. VPS35/29/26 and Rab7 colocalise on endosomal membranes. Cells expressing either GFP-Rab7 (A-C) or GFP-Rab7Q67L (D-F) were grown in 60 mm dishes, washed and then snap frozen to permeabilise them. After fixation, the cells were labelled with anti-VPS26 and anti-GFP antibodies followed by 5 nm anti-rabbit IgG colloidal gold and 10 nm anti-mouse IgG colloidal gold. The cells were then fixed again, embedded in resin and sectioned for EM. The gold particles have been false colour coded to aid the distinction between the 5 nm and 10 nm colloidal gold. The 5 nm particles are coloured blue and the 10 nm particles are yellow. VPS26 and GFP-Rab7 or GFP-Rab7Q67L colocalise extensively. Scale bar: 250 nm.

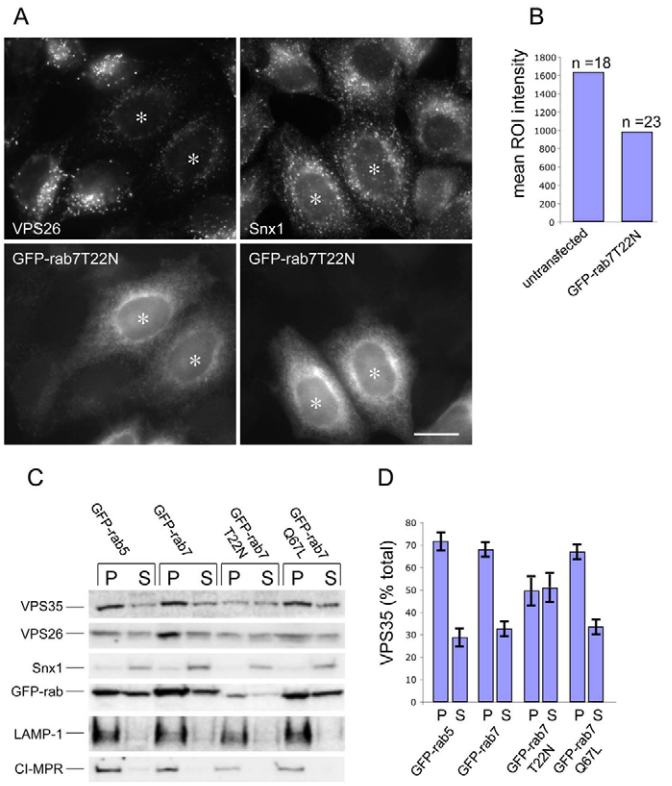

Fig. 3. The GDP-locked Rab7T22N mutant inhibits VPS26 membrane association. (A) Cells stably expressing GFP-Rab7T22N were seeded with untransfected HeLa cells onto cover slips before fixation and labelling with anti-VPS26 or anti-Snx1 antibodies. Cells expressing the GFP-Rab7T22N mutant (*) display reduced VPS26 localisation but Snx1 is unaffected. Scale bar: 20 μm. (B) The fluorescence intensity of the VPS26 labelling was quantified within a perinuclear region of interest (ROI). Cells expressing the GFP-Rab7T22N mutant had ~40% less intense VPS26 labelling. (C) Cells expressing GFP-Rab5, GFP-Rab7, GFP-Rab7T22N or GFP-Rab7Q67L were snap frozen to permeabilise them, washed and scraped into buffer before centrifugation to pellet the membranes. Pellet (P) and supernatant (S) samples were subjected to SDS-PAGE and analysed by western blotting. (D) The amount of VPS35 in the pellet (P) and supernatant (S) fractions from two western blots was quantified and the average is shown graphically expressed as a percentage of the total in the cell-line assayed. VPS35 is ~70% membrane associated except in cells expressing the Rab7T22N mutant where VPS35 is <50% membrane associated. Error bars represent s.e.m.

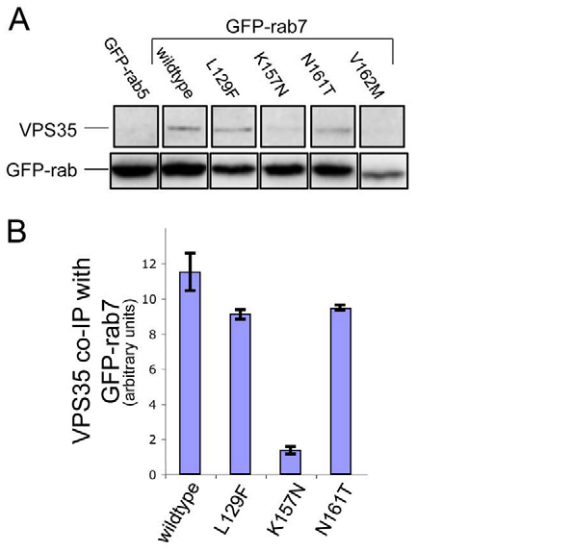

Fig. 4. The Rab7K157N CMT mutant does not interact with VPS35/29/26. (A) Cells stably expressing GFP-Rab5, GFP-Rab7, GFP-Rab7L129F, GFP-Rab7K157N, GFP-Rab7N161T and GFP-Rab7V162M were treated with nocodazole before lysis and incubation with anti-GFP antibody. After washing, the immunoprecipitated proteins were subjected to SDS-PAGE and analysed by western blotting. VPS35 did not co-immunoprecipitate with GFP-Rab5 but did co-immunoprecipitate with GFP-Rab7, GFP-Rab7L129F and GFP-Rab7N161T. VPS35 only weakly interacted with GFP-Rab7K157N. (B) The data from two experiments were quantified by densitometry (normalising to the respective GFP-Rab7 signal) and the average is shown graphically. Error bars represent s.e.m.

untransfected HeLa cells and then labelled with antibodies against either VPS26 or sorting nexin 1 (Snx1). Cells expressing the T22N mutant (Fig. 3A, asterisk) have significantly less punctate endosomal VPS26 (relative to untransfected cells) whereas the Snx1 labelling was unaffected. By measuring the fluorescence intensity of the VPS26 labelling within a perinuclear region of interest (ROI) in untransfected or cells expressing GFP-Rab7T22N, a decrease of ~40% in fluorescence intensity of VPS26 labelling was observed in GFP-Rab7T22N cells (Fig. 3B).

The data from Fig. 3A suggest that there is less membrane-associated VPS26 in cells expressing the GFP-Rab7T22N mutant. This was further investigated using an assay to quantitatively determine the amount of membrane-associated retromer. Cells were quick frozen and thawed to permeabilise them and then scraped up into buffer before centrifugation to pellet the cells and the internal membranes. Pellet (P) and supernatant (S) fractions were analysed for VPS35 and VPS26 by western blotting (see Fig. 3B). The membrane proteins LAMP1 and CI-MPR were detected in the pellet fractions, indicating that permeabilisation does not cause leakage of membranes into the supernatant fraction. In most samples, VPS35 and VPS26 were predominantly membrane associated, unlike Snx1, which was detected in the cytosolic supernatant fraction, indicating that Snx1 membrane association is somewhat labile. In cells expressing the GFP-Rab7T22N mutant, there is a marked reduction of membrane-associated VPS35 and VPS26. The amount of VPS35 present in the pellet (membrane) and supernatant (cytosol) fractions was quantified by densitometry and is shown in Fig. 3C. In cells expressing GFP-Rab5, GFP-Rab7 or GFP-Rab7Q67L there was ~70% of the VPS35 in the pelletable membrane fraction compared with <50% in the cells expressing GFP-Rab7T22N, even though there was relatively poor expression of the GFP-Rab7T22N construct compared with the other GFP-Rab constructs (see Fig. 3B).

Mutations in Rab7 have been shown to cause a variant of the neurodegenerative disorder, Charcot-Marie-Tooth (CMT) disease. Four single amino acid Rab7 mutations have been described in patients with CMT type 2B; L129F, K157N, N161T and V162M (Verhoeven et al., 2003; Houlden et al., 2004; Meggouh et al., 2006). To determine whether the CMT-causing mutations affect the interaction with between Rab7 and the VPS35/29/26 complex in vivo, we performed native immunoprecipitations from cells stably expressing GFP-tagged versions of the mutant Rab7 proteins (Fig. 4A). VPS35 weakly co-immunoprecipitated with GFP-Rab7K157N, but interacted normally with the L129F and N161T mutants. The V162M mutant was poorly expressed and therefore it is not possible

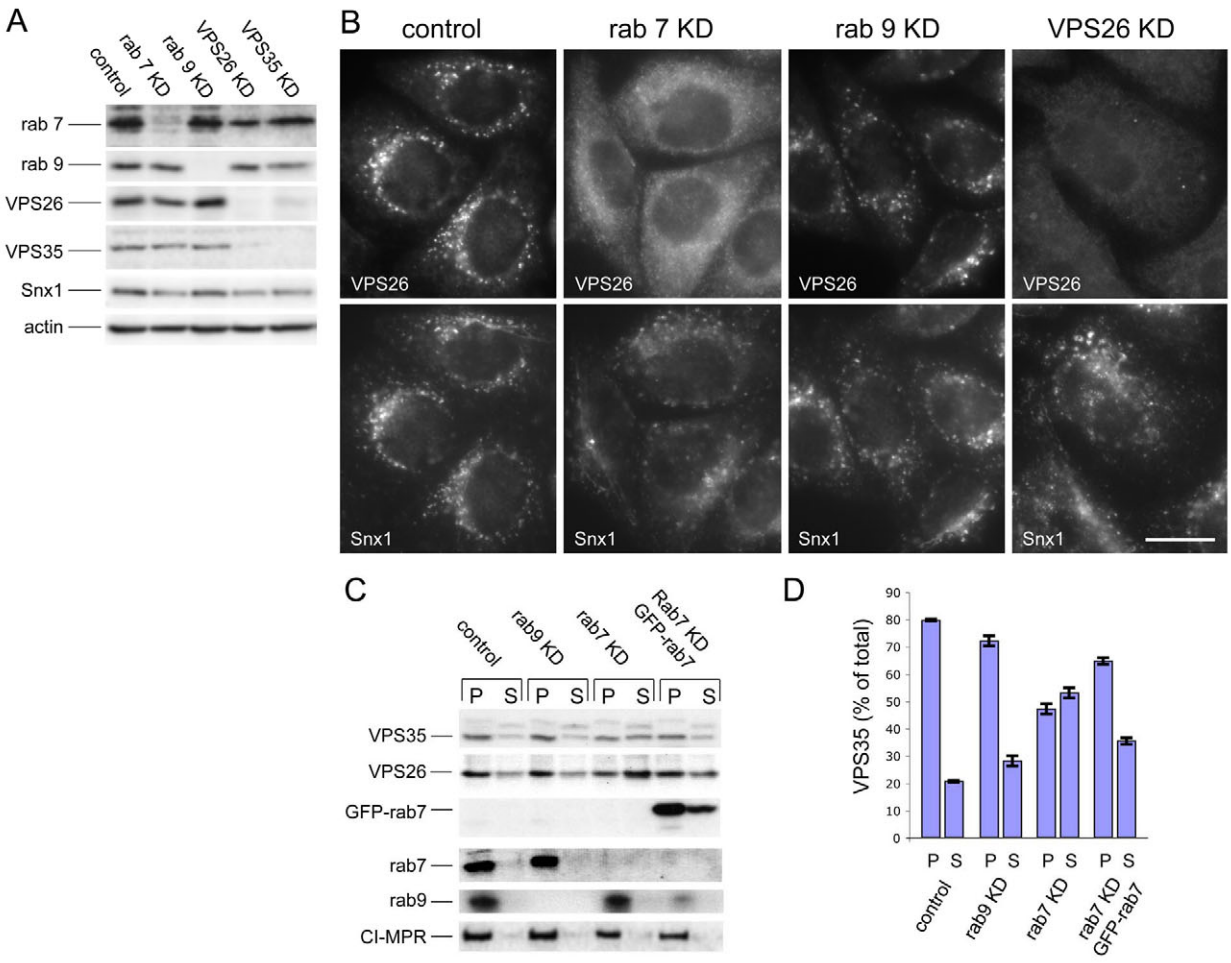

Fig. 5. Loss of Rab7 expression results in VPS26 redistribution to the cytoplasm. (A) Lysates from cells treated with siRNA to knock down (KD) expression of Rab7, Rab9, VPS26 or VPS35 were analysed by western blotting. The siRNA abolished expression of the respective target gene. (B) Cells treated with siRNA in A were labelled with antibodies against VPS26 and Snx1. Loss of Rab7 expression results in VPS26 becoming cytosolic whereas Snx1 remains membrane associated. Loss of Rab9 expression did not produce a similar effect. Scale bar: 20 µm. (C) The amount of membrane associated VPS35 and VPS26 was determined quantitatively using the same assay in Fig. 3B. Loss of Rab7 expression results in a notable shift of VPS35 and VPS26 into the cytosolic fraction. The effect is rescued by expression of GFP-Rab7. (D) The amount of VPS35 in the pellet (P) and supernatant (S) fractions from two western blots was quantified and the average is shown graphically expressed as a percentage of the total in the cell line assayed. 70-80% of VPS35 is membrane associated, except in cells treated with siRNA to silence Rab7 expression, where <50% of VPS35 is membrane associated. Error bars represent s.e.m.

to draw any conclusions regarding its ability to interact with VPS35/29/26. Data from two native immunoprecipitation experiments were quantified and normalised to the expression of the respective GFP-Rab7 protein and the amount of VPS35 interacting with the respective GFP-Rab7 is shown in Fig. 4B.

VPS35/29/26 membrane association requires Rab7

What is the function of the VPS35/29/26-Rab7 interaction? This question was addressed using siRNA to knock down Rab7 expression. As an additional control, siRNA was used to knock down Rab9. In Fig. 5A, cell lysates from control, Rab7, Rab9, VPS26 or VPS35 knockdowns are shown confirming that treatment with the respective siRNA was able to ablate expression of the target gene. It is worth noting that loss of VPS26 causes VPS35 to be unstable and vice-versa, whereas loss of Rab7 or Rab9 did not significantly affect levels of the VPS35 or VPS26 proteins. When the siRNA-knockdown cells were analysed by fluorescence microscopy it was observed that VPS26 localisation was severely perturbed in the Rab7-knockdown cells but not in the Rab9-knockdown cells (Fig. 5B). Snx1 localisation was affected in Rab7-knockdown cells, but not as dramatically as VPS26 localisation. Loss of Rab7 expression appeared to redistribute VPS26 into the cytoplasm. To quantitatively examine the membrane association of VPS35 and VPS26 after loss of Rab7 expression, cells treated with siRNA to knock down Rab7 or Rab9 were then subjected to the quick freeze-thaw protocol to assay for membrane-associated or cytoplasmic VPS35 and VPS26. In Fig. 5C, pellet (P) and supernatant (S) samples were western blotted for VPS35, VPS26, Rab7, Rab9 and the CI-MPR. Loss of Rab7 expression resulted in a significant shift of both VPS35 and VPS26 into the supernatant fraction, consistent with a redistribution of these proteins into the cytoplasm. Rab9 knockdown had little effect, and the effect of the loss of endogenous Rab7 can be rescued by expression of the GFP-tagged Rab7 from mouse, which was resistant to the siRNA targeting human Rab7 in the HeLa cells used in this study. The data from two western blots was quantified and is shown in Fig. 5D.

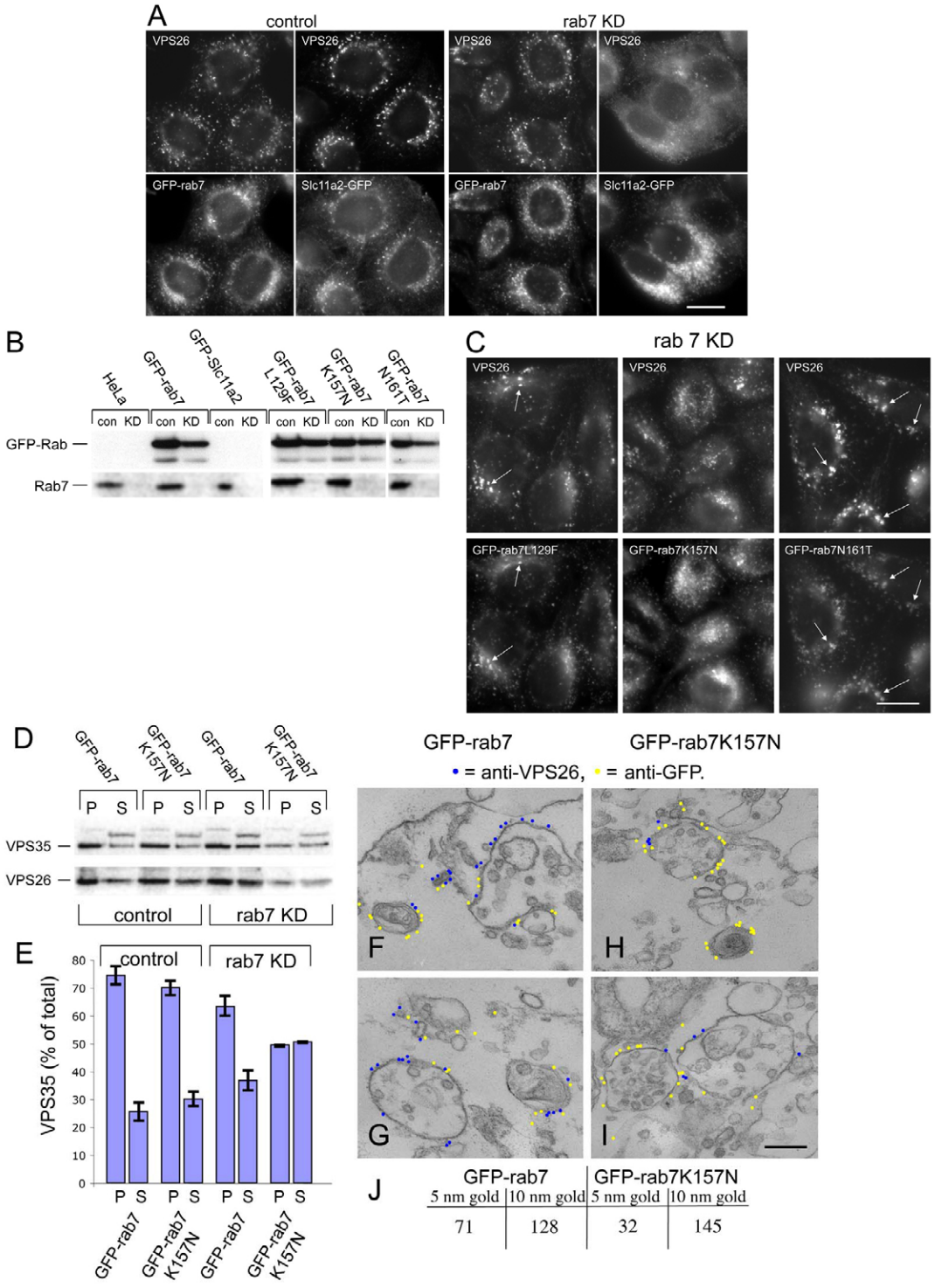

Fig. 6. GFP-Rab7 can rescue the loss of endogenous Rab7. (A) Cells expressing GFP-Rab7 or the endosomal membrane protein Slc11a2-GFP were treated with siRNA to knock down Rab7. Expression of GFP-Rab7 was able to rescue VPS26 localisation but expression of Slc11a2-GFP does not rescue VPS26 redistribution to the cytoplasm. Scale bar: 20 µm. (B) Control (con) or knockdown (KD) lysates from untransfected HeLa cells or cells expressing GFP-Rab7, Slc11a2-GFP, GFP-Rab7L129F, GFP-Rab7K157N or GFP-Rab7N161T, which had been treated with siRNA to knock down Rab7 expression were western blotted for Rab7 or the respective GFP-Rab7 protein. (C) The localisation of VPS26 in cells expressing GFP-Rab7L129F, GFP-Rab7K157N or GFP-Rab7N161T, which had been treated with siRNA to knock down Rab7 (see B) was investigated by immunofluorescence. Scale bar: 20 µm. (D) The Rab7K157N mutant results in less membrane-associated VPS35 and VPS26. Cells expressing GFP-Rab7 or GFP-Rab7K157N were treated with siRNA to knock down endogenous Rab7 expression and were then analysed using a centrifugation assay to measure membrane-associated VPS35 and VPS26. (E) Results from the western blot (D) were quantified and are shown graphically. Error bars represent s.e.m. (F-I) Rab7 expression was ablated in cells expressing GFP-Rab7 (F,G) or GFP-Rab7K157N (H,I) and the cells were then prepared for pre-embedding labelling EM. VPS26 labelling (5 nm gold, coloured blue) colocalises with anti-GFP (10 nm gold, coloured yellow) in GFP-Rab7 cells but there is little VPS26 labelling observed in GFP-Rab7K157N cells. Scale bar: 250 nm. (J) Gold particles from six micrographs each of GFP-Rab7 and GFP-Rab7K157N expressing cells were counted confirming that there is a marked reduction in VPS26 labelling.

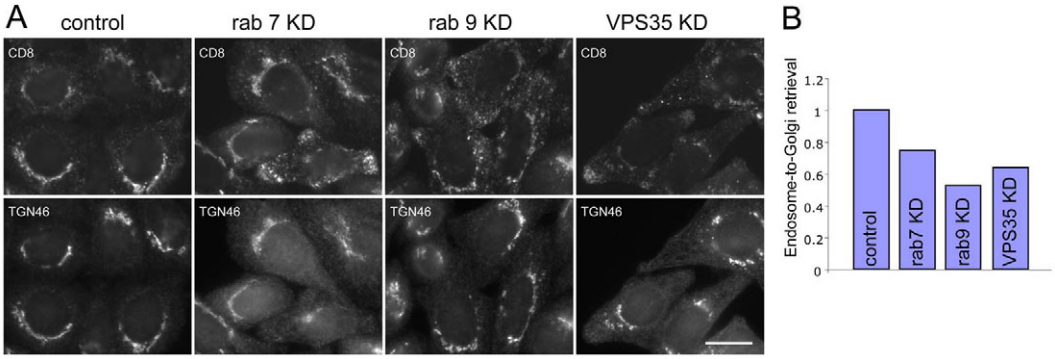

Fig. 7. Loss of Rab7 expression causes an endosome-to-Golgi retrieval defect. (A) Cells expressing the CD8-CIMPR reporter protein were treated with siRNA to knock down Rab7, Rab9 or VPS35. The cells were incubated with anti-CD8 at 4°C and then warmed to 32°C for 24 minutes before fixation and labelling with anti-TGN46 followed by appropriate fluorescent secondary antibodies. Loss of Rab7 expression results in a partial block in endosome-to-Golgi retrieval. Scale bar: 20 µm. (B) The microscopy-based endosome-to-Golgi retrieval assay was quantified by determining the extent of colocalisation of between endocytosed anti-CD8 and TGN46 relative to the total anti-CD8 fluorescence. The efficiency of endosome-to-Golgi retrieval in the knockdown cells is expressed relative to the control cells.

The ability of the GFP-Rab7 to rescue the VPS26-redistribution phenotype observed in Rab7-knockdown cells was further explored by fluorescence microscopy. Cells expressing GFP-Rab7 or a GFP-tagged endosomal membrane protein, Slc11a2 (Lam-Yuk-Tseung and Gros, 2006), were labelled with antibodies against VPS26 (Fig. 6A, left panels). Slc11a2-GFP was used as a control in this experiment because it is localised to endosomes, GFP-tagged and expressed from the same vector as GFP-Rab7. Using siRNA, Rab7 expression in GFP-Rab7 or cells expressing Slc11a2-GFP was ablated. As shown in Fig. 6A (right hand panels), VPS26 localisation was normal in cells expressing GFP-Rab7, but was redistributed to the cytoplasm in cells expressing Slc11a2. This confirms that GFP-Rab7 can rescue the loss of endogenous Rab7 and that the rescue is specific to GFP-Rab7 because Slc11a2-GFP did not rescue loss of Rab7. In Fig. 6B, lysates from control and knockdown cells were analysed to confirm that treatment with the Rab7 siRNA did ablate Rab7 expression.

As the GFP-Rab7 was able to rescue the VPS26-redistribution phenotype, we next examined whether the CMT Rab7 mutants could also rescue VPS26 redistribution after loss of endogenous Rab7. Lysates from cells expressing GFP-Rab7L129F, K157N or N161T were western blotted for Rab7 after Rab7 knockdown (Fig. 6B) and the localisation of VPS26 in cells where the only Rab7 is a mutant Rab7 was determined by immunofluorescence (Fig. 6C). VPS26 appeared to be membrane associated after loss of Rab7, even in cells expressing the Rab7K157N mutant that weakly co-immunoprecipitates with VPS35 (see Fig. 4), although there are qualitative differences between the VPS26-labelled structures in the GFP-Rab7K157N cells and the other two mutants, and relatively little colocalisation between the GFP-Rab7K157N mutant and VPS26, although colocalisation was observed between VPS26 and GFP-Rab7L129F and GFP-Rab7N161T (indicated by arrows in Fig. 4).

When the amount of membrane-associated VPS26 and VPS35 was measured using the centrifugation assay, it was observed that although GFP-Rab7 could rescue the loss of endogenous Rab7, the GFP-Rab7K157N did not rescue VPS35 and VPS26 membrane association indicating that VPS35 and VPS26 are more prone to dissociating from the membrane when the only Rab7 present is the K157N mutant (Fig. 6D,E). Furthermore, when cells expressing GFP-Rab7 or GFP-Rab7K157N were treated with siRNA to knock down endogenous Rab7 and then analysed by EM, it was observed that there was colocalisation between the GFP-Rab7 (Fig. 6F,G, yellow) and VPS26 (Fig. 6F,G, blue), but there was relatively little

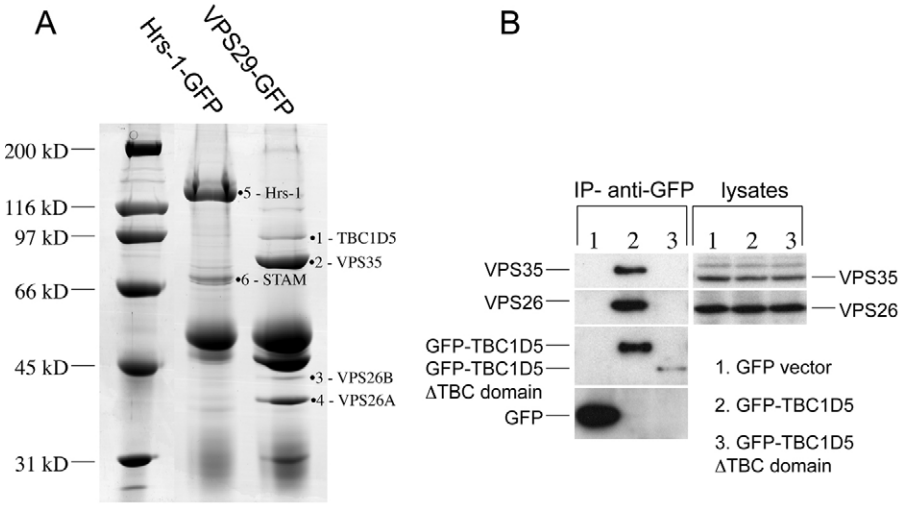

Fig. 8. Identification of a novel retromer-interacting protein, TBC1D5. (A) Cells expressing either Hrs-1-GFP or VPS29-GFP were washed, lysed and then incubated with anti-GFP and protein-A-Sepharose to immunoprecipitate the respective GFP-tagged protein. After washing, the proteins were eluted at low pH, acetone precipitated, and subjected to SDS-PAGE and mass spectrometry. (B) GFP-tagged TBC1D5 was transiently transfected into HeLa cells along with empty vector and the truncation of TBC1D5 that lacks the TBC domain. 24 hours after transfection, the cells were lysed and immunoprecipitated with anti-GFP and analysed by western blotting. VPS35 and VPS26 co-immunoprecipitated with GFP-TBC1D5 but not GFP alone or the ΔTBC domain construct.

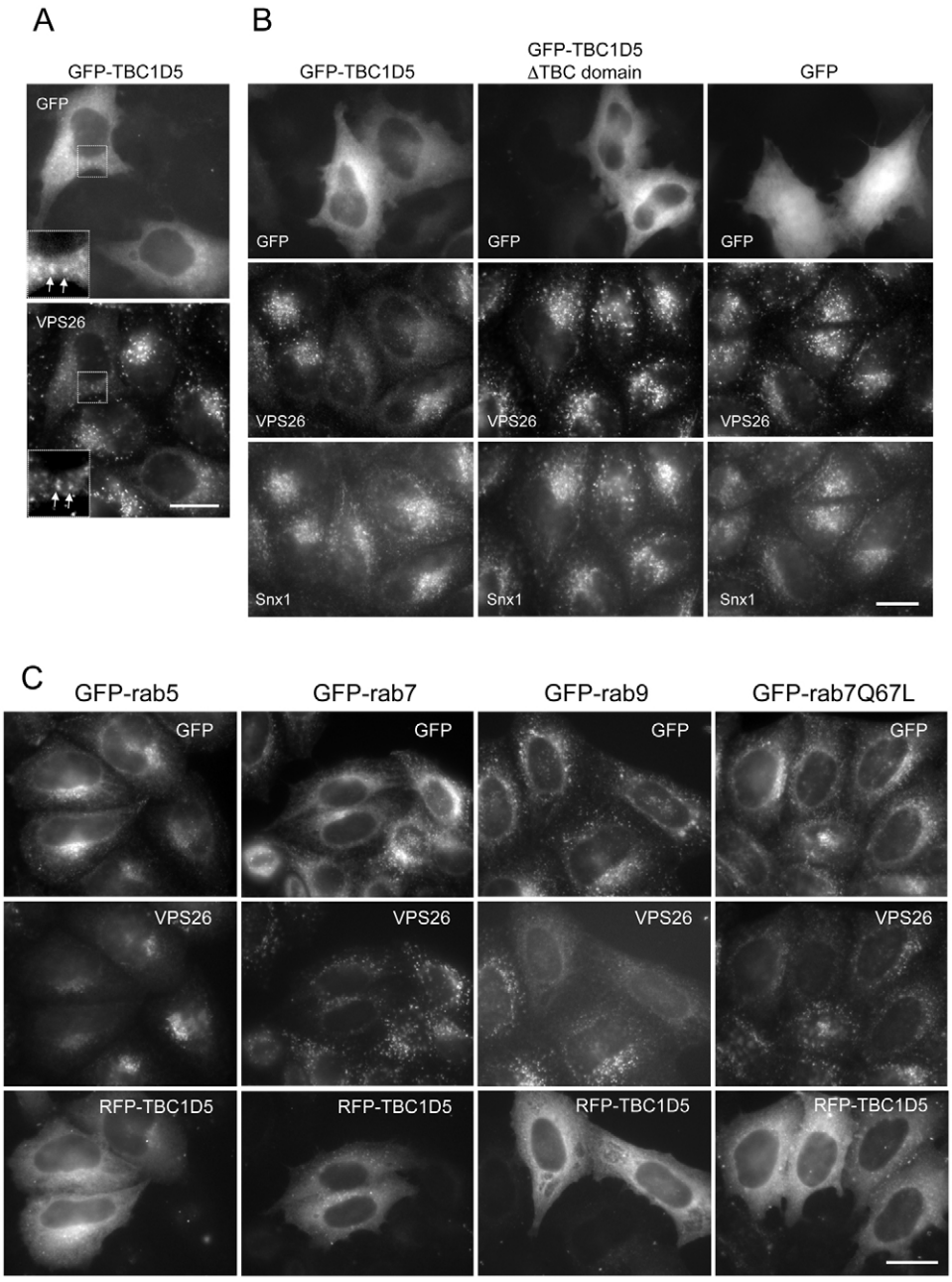

Fig. 9. Expression of TBC1D5 negatively regulates VPS26 recruitment. (A) Cells transiently transfected with GFP-TBC1D5 were fixed and labelled with anti-VPS26 antibodies. GFP-TBC1D5 is predominately cytosolic but colocalisation with VPS26 can be observed occasionally (see inset box). Scale bar: 20 μm. (B) Cells were transiently transfected with GFP-TBC1D5, the ΔTBC domain construct or GFP alone. After fixation, cells were labelled with antibodies against VPS26 or Snx1. Overexpression of TBC1D5 results in reduced VPS26 labelling but has no effect on Snx1 localisation. The ΔTBC domain or GFP alone had no effect. Scale bar: 20 μm. (C) Cells expressing GFP-Rab5, GFP-Rab7, GFP-Rab9 or GFP-Rab7Q67L were transiently transfected with red fluorescent protein (RFP)-TBC1D5, fixed and then labelled with anti-VPS26 antisera. Overexpression of TBC1D5 can redistribute GFP-Rab7 into the cytoplasm but does not affect GFP-Rab5, GFP-Rab9 or the Rab7Q67L mutant. Scale bar: 20 μm.

membrane-associated VPS26 present in the GFP-Rab7K157N mutant, and almost no colocalisation was observed (Fig. 6H,I). Gold particles were counted in six micrographs from cells expressing GFP-Rab7 and GFP-Rab7K157N, and the data are shown in Fig. 6J. In the cells expressing GFP-Rab7K157N, only thirty-two 5 nm gold particles (anti-VPS26) were counted whereas in the cells expressing GFP-Rab7, seventy-one 5 nm gold particles were counted.

Loss of Rab7 results in VPS26 and VPS35 becoming cytoplasmic and would therefore be expected to reduce the efficiency of endosome-to-Golgi retrieval. Cells expressing a CD8-CIMPR reporter protein were treated with siRNA to knock down either Rab7, Rab9 or VPS35 and then analysed for endosome-to-Golgi retrieval efficiency (Fig. 7A), using an antibody-uptake assay we have used previously (Seaman, 2004; Seaman, 2007; Gokool et al., 2007). Loss of Rab7 results in an endosome-to-Golgi retrieval defect although the effect is less striking than the loss of Rab9 or VPS35. When the assay was quantified by determining how much endocytosed anti-CD8 colocalises with TGN46, a marker protein for the TGN, loss of Rab7 resulted in ~25% defect whereas Rab9 ablation caused a ~50% defect (Fig. 7B). Knockdown of VPS35 produced an effect intermediate to that seen with knockdown of Rab7 or Rab9.

The Rab-GAP protein TBC1D5 interacts with the VPS35/29/26 complex

The data shown so far is consistent with Rab7 performing a regulatory role in the recruitment of VPS35/29/26 to the membrane.

Could retromer be interacting with other factors to regulate its recruitment? To address this question, a native immunoprecipitation was performed on cells expressing VPS29-GFP. Cells expressing VPS29-GFP were lysed and treated with anti-GFP (Fig. 8A). Cells expressing a GFP-tagged construct of the ESCRT complex protein Hrs-1 were used as a control because Hrs-1 is endosomally localised similarly to VPS29 (Bache et al., 2003). After the GFP-tagged proteins were immunoprecipitated, the samples were subjected to SDS-PAGE and mass spectrometry. The detailed results of mass spectrometry are shown in supplementary material Table S2. One protein that was identified in the VPS29-GFP lane was of significant interest, namely TBC1D5. The TBC family of proteins function as Rab-GAPs and regulate Rab activity by stimulating GTP hydrolysis (Pan et al., 2006). A GFP-TBC1D5 construct was generated and then transiently transfected into HeLa cells before lysis. Anti-GFP was used to immunoprecipitate the lysates. The GFP-TBC1D5 construct was able to immunoprecipitate both VPS26 and VPS35 (Fig. 8B), confirming the interaction observed in Fig. 8A. Empty vector does not co-immunoprecipitate any retromer proteins and neither does a truncated version of GFP-TBC1D5 that is missing the TBC domain, although this construct was poorly expressed compared with full-length GFP-TBC1D5.

When the GFP-TBC1D5 was transiently transfected into HeLa cells, it was observed that the protein was mainly cytoplasmic but some modest colocalisation with VPS26 was also observed (Fig. 9B). More strikingly, cells expressing the GFP-TBC1D5 protein demonstrated significantly less membrane-associated VPS26, but Snx1 was unaffected (Fig. 9B). This is an identical effect to that observed in cells expressing the dominant negative GFP-Rab7T22N mutant (see Fig. 2A). The GFP-TBC1D5 ΔTBC domain did not produce the same effect and neither did empty vector that expressed GFP alone.

If the overexpression of TBC1D5 was causing VPS26 to dissociate from the membrane, was it affecting the membrane association of Rab7? This question was investigated by transfection of a red fluorescent protein (RFP)-TBC1D5 construct. Cells stably expressing either GFP-Rab5, GFP-Rab7, GFP-Rab9 or GFP-Rab7Q67L were transiently transfected with RFP-TBC1D5 and then analysed by fluorescence microscopy (Fig. 9C). The RFP-TBC1D5 expression resulted in VPS26 labelling becoming weak and diffuse but did not alter the localisation of GFP-Rab5 or GFP-Rab9. We did, however, observe an effect of RFP-TBC1D5 on the localisation of GFP-Rab7, which no longer appeared to be associated with punctate structures. The GFP-Rab7Q67L mutant, which is GTP-locked because of a mutation in the critical glutamine residue required for GAP-stimulated GTP hydrolysis (Pan et al., 2006), appeared to be resistant to the effects of the RFP-TBC1D5, and it remained associated with the punctate structures observed in both transfected and adjacent non-transfected cells. Transient expression of RFP-TBC1D5 in cells expressing VPS29-GFP resulted in reduced labelling of VPS29-GFP and VPS26 whereas in Hrs-1-GFP-expressing cells, VPS26 membrane association was reduced, but the Hrs-1-GFP labelling was unchanged, indicating that the RFP-TBC1D5 exerted its effects on VPS35/29/26 and not on Hrs-1, another endosomal protein (supplementary material Fig. S3).

Discussion

In this study, we investigated the functional significance of the interaction between the cargo-selective retromer complex (VPS35/29/26) and the small GTPase Rab7. We show that VPS35/29/26 interacts with Rab7 but not with Rab5 or Rab9. The interaction between VPS35/29/26 and Rab7 is substoichiometric, which is consistent with a transient and/or dynamic interaction. Mass spectrometric analysis of the large-scale native immunoprecipitations confirmed that the VPS35/29/26 complex interacts with Rab7 and also indicated that the interaction is likely to be direct, because the only other proteins that were detected in the GFP-Rab7 immunoprecipitation lane were Rab escort protein-1 and GDI-1 and GDI-2, both of which are involved in maintaining the cytosolic Rab7 in a soluble form (Goody et al., 2005). We did not observe a band corresponding to VPS29 in the native immunoprecipitation samples, possibly because the silver stain used to visualise the bands does not stain the VPS29 protein. Attempts to investigate the interaction between Rab7 and VPS35/29/26 using the yeast two-hybrid system were unsuccessful, possibly because Rab7 interacts with the assembled VPS35/29/26 trimer and therefore the interaction cannot be reproduced using systems that measure interactions between individual proteins.

Cells expressing the GDP-locked Rab7T22N mutant demonstrated ~40% reduced intensity of the VPS26 labelling compared with untransfected cells, but the labelling of Snx1 was unaffected. Likewise, when Rab7 expression was ablated using siRNA, the VPS26 labelling was dramatically altered, and appeared to be cytoplasmic and diffuse. Rather than relying solely on immunofluorescence data to determine the extent of the membrane association of VPS35/29/26, we developed a simple assay to measure the amount of membrane-associated VPS35 and VPS26. This assay indicated that in untransfected cells or cells stably expressing GFP-Rab5, GFP-Rab7 or GFP-Rab7Q67L, VPS35 and VPS26 are ~70-80% membrane associated. This value corresponds well with the amount of membrane-associated Vps35p and Vps26p in yeast (Reddy and Seaman, 2001). In cells expressing the Rab7T22N mutant, or cells in which Rab7 expression had been lost, there was a shift of VPS26 and VPS35 into the cytosolic fraction, consistent with the reduction in VPS26 fluorescence intensity observed.

Loss of Rab7 does not, however, result in a total shift of VPS26 and VPS35 into the cytosolic fraction and does not cause a total block in endosome-to-Golgi retrieval. This suggests that loss of Rab7 leads to the VPS35/29/26 complex becoming less stably associated with the membrane, but still able to recruit to the membrane to sort cargo, albeit inefficiently.

The disease-causing K157N mutant does not interact with VPS35/29/26 in native immunoprecipitations, but can rescue the loss of Rab7 when the membrane association of VPS26 is examined by immunofluorescence. However, in cells where the only Rab7 present is the K157N mutant, VPS26 and VPS35 are weakly membrane associated and become cytosolic when the cells are permeabilised. This is the first report of a significant loss of function for the CMT Rab7K157N mutant, and hints that the underlying cause of the neuronal degeneration in patients with this version of CMT might be linked to the role of retromer in regulating endosomal membrane protein sorting. As the Rab7K157N mutant is an autosomal dominant mutation, there will still be wild-type Rab7 present in CMT patients carrying the K157N mutation, so perhaps the presence of the K157N mutation affects the kinetics of VPS35/29/26 recruitment leading to reduced efficiency of endosomal protein sorting, which could be deleterious in the very long axons that are affected in CMT patients.

How does Rab7 regulate VPS35/29/26 recruitment? The data presented here are consistent with the hypothesis that Rab7 can

catalyse the recruitment of VPS35/29/26 to endosomal membranes. The interaction between the cargo-selective retromer sub-complex and Rab7 might contribute to the targeting and recruitment of VPS35/29/26 to endosomal membranes but it seems likely that additional interactions help to stabilise the membrane association of the VPS35/29/26 complex. These interactions could be with cargo proteins such as the CI-MPR or a SNARE protein or with proteins such as the sorting nexins (e.g. Snx1 and Snx2) that are important components in the endosome-to-Golgi pathway (Carlton et al., 2004; Rojas et al., 2007). Alternatively, the additional interactions could be with the membrane itself. One way in which Rab7 could catalyse VPS35/29/26 recruitment is through lipid modifying enzymes. Rab7 interacts with PtdIns 3-kinase, which is required for the membrane recruitment of Snx1 via the PtdIns3*P*-binding PX domain present in Snx1 (Stein et al., 2003). In our experiments, treatment with wortmannin to inhibit PtdIns 3-kinase activity causes Snx1 to dissociate from the membrane but does not abolish the membrane association of VPS26 (supplementary material Fig. S4). This suggests that PtdIns 3-kinase activity is not essential for VPS26 recruitment.

Whilst this manuscript was in preparation, Bonifacino and colleagues published their own observations that Rab7 interacts with retromer to regulate the recruitment of retromer to the endosomal membrane (Rojas et al., 2008). Our data is in broad agreement with theirs, except that we do not find that loss of Rab7 expression results in all VPS35/29/26 becoming cytosolic and that loss of Rab7 does not cause a complete block in endosome-to-Golgi retrieval as they report. As the report from Rojas and colleagues did not quantify either the membrane association of retromer or the endosome-to-Golgi retrieval defect after loss of Rab7, it is possible that the discrepancies are simply due to their lack of quantitative data.

Rab7 has traditionally been viewed as a marker for 'late' endosomes (Zerial and McBride, 2001) and yet retromer has been shown to localise to Rab5-positive 'early' endosomes (Seaman, 2004; Popoff et al., 2007). This apparent contradiction can be resolved if the endocytic system is viewed as a continuum of maturing organelles rather than only 'early' and 'late' endosomes (Bonifacino and Rojas, 2006). This view of endosomal membrane dynamics is consistent with observations that Rab5 and Rab7 can co-exist on the same population of endosomal membranes (Rink et al., 2005). It is on such Rab5- or Rab7-positive membranes where we would predict that the bulk of retromer is localised and from where endosome-to-Golgi retrieval will occur.

We did not detect any interaction between VPS35/29/26 and Rab9, although it is well established that Rab9 has a prominent role in endosome-to-Golgi retrieval (Reiderer et al., 1994). This might be because Rab9 functions downstream of retromer or because Rab9 acts in a parallel pathway. Further work is required to elucidate the relationship between retromer and Rab9.

In addition to Rab7 interacting with VPS35/29/26, we have identified another retromer-interacting protein by native immunoprecipitation and mass spectrometry. The TBC-domain-containing protein, TBC1D5, co-immunoprecipitates with VPS29-GFP, but not with GFP-tagged Hrs-1. Interestingly, a genome-wide protein-protein interaction study in *Drosophila* has reported an interaction between fly VPS29 (CG4764) and the fly homologue of TBC1D5 (namely CG8449) (Giot et al., 2003). Overexpression of GFP-TBC1D5 results in VPS26 being displaced from the membrane in a similar fashion to the expression of GFP-Rab7T22N. When the effect of TBC1D5 overexpression on the GFP-labelled Rab proteins was investigated, it was observed that GFP-Rab5 and Rab9 were unaffected by TBC1D5 but GFP-Rab7 appeared displaced from the membrane. The membrane association of the Q67L Rab7 was unaffected by expression of TBC1D5.

These data indicate the TBC1D5 could act as a GAP for Rab7, although we cannot rule out the possibility that the effect we observed of TBC1D5 overexpression upon Rab7 localisation could be due to indirect effects. However, in agreement with our data, the homologue of TBC1D5 in the nematode *Caenorhabditis elegans* (encoded by the RBG-3 gene) has been shown to act as a GAP with a strong preference for nematode Rab7 (Mukhopadhyay et al., 2007). In summary, we propose a model for the recruitment of the cargo-selective retromer complex in which Rab7 'primes' the membrane to promote VPS35/29/26 recruitment to sort cargo such as the CI-MPR. As VPS35/29/26 is recruited to the membrane, the Rab-GAP TBC1D5 is also recruited, which can then trigger the release of Rab7 and VPS35/29/26 from the membrane. The in vivo action of TBC1D5 on Rab7 might be strictly limited to sites where VPS35/29/26 is present, thereby allowing Rab7 to regulate fusion of endosomes with lysosomes at other sites within the endocytic pathway. This means that retromer is similar to other vesicle coat complexes, such as COPII and coatomer/COPI, in that it interacts with a GAP that serves to downregulate the membrane association of the respective vesicle coat, thereby generating a regulatory feedback loop that underlies the dynamic nature of coat-membrane interactions.

Materials and Methods

General reagents

Biochemicals were purchased from Sigma (Poole, UK). Molecular biology reagents were purchased from New England Biolabs (Hitchin, UK). ^{125}I-protein A used in western blotting was supplied by either Amersham Biosciences (St Albans, UK) or Perkin Elmer (Waltham, MA).

Antibodies

Anti-VPS26 and anti-VPS35 antisera have been described previously (Seaman, 2004). Snx1 was detected using either polyclonal antisera described previously (Seaman, 2004) or a monoclonal antibody purchased from BD BioScience (Oxford, UK). Polyclonal antisera against Rab9, TGN46 and GFP were raised in rabbits using GST-fusion proteins as antigens. All polyclonal antisera were affinity purified before use. Monoclonal anti-Rab7 was purchased from Sigma, as was the monoclonal anti-GFP used for electron microscopy. The monoclonal anti-CD8 was produced from a hybridoma cell line obtained from the ATCC and is described elsewhere (Seaman, 2007).

Molecular biology and other standard procedures

GFP-Rab constructs have been described previously (Seaman, 2004). These constructs were subcloned into pIRESneo2 (Clontech, Paisley, UK) and stable cells lines expressing the various GFP-Rab constructs were generated. Mutations in the Rab7 cDNA were produced using the QuikChange kit (Stratagene, La Jolla, CA) following manufacturer's instructions. The cDNA for TBC1D5 (KIAA0210) was obtained from the Kazusa Human cDNA project (Japan) and was amplified by PCR to add a *Bam*HI site at the 5′ end and a *Sal*I site at the 3′ prime end so that the PCR products could be cloned into pEGFP C1 vector (Clontech). The TBC domain was excised from the GFP-TBC1D5 construct by digestion with *Pst*I and religation. The GFP-tagged Slc11a2 construct was provided by Jennie Blackwell (CIMR, Cambridge, UK) and is described by Eichner-Techau et al. (Eichner-Techau et al., 2007). It was subcloned into pIRESneo2 (Clontech), transfected in HeLa cells and stably expressing cells were selected using G418.

DNA transfections were performed using Effectene (Qiagen, Crawley, UK) following the manufacturer's instructions. Small interfering (si) RNA transfections were performed as previously described (Seaman, 2004). Immunofluorescence, SDS-PAGE and western blotting were, respectively, performed as previously described (Seaman, 2004; Reddy and Seaman, 2001). Endosome-to-Golgi retrieval assay using CD8-CIMPR cells and anti-CD8 was performed and quantified as described (Gokool et al, 2007).

Fluorescence microscopy

Immunofluorescence microscopy was performed using a Zeiss Axioplan epifluorescence microscope with a Zeiss plan-apochromat 63× oil-immersion lens at room temperature. The images were obtained using a Princeton Instruments CCD

camera, which was controlled via Scanalytics IP labs software. Images were cropped using Adobe Photoshop software. Fluorescence intensity was measured using the Scanalytics IP lab software. The efficiency of endosome-to-Golgi retrieval was determined by using the Scanalytics IP lab software to measure the number of anti-CD8 pixels that were coincident with TGN46 and the total number of anti-CD8 pixels for the respective cell. The TGN46 coincident pixels divided by the total pixels provides a measurement of the extent of retrieval. A minimum of ten cells was quantified and a mean value for endosome-to-Golgi obtained. This value in control cells was assigned an arbitrary value of 100% and the value in the respective KD cells is expressed as a ratio of the control.

Electron microscopy

The pre-embedding labelling procedure used was essentially as described (Seaman, 2004) with some minor modifications. The cells were washed in PBS, snap frozen using liquid nitrogen and then thawed rapidly on the bench. The cells were then washed with 1 ml PBS before fixation with 4% paraformaldehyde in PBS. After fixation, the cells were blocked with 3% BSA in PBS and labelled with rabbit antibodies against VPS26 and mouse anti-GFP. 5 nm anti-rabbit colloidal gold and 10 nm anti-mouse colloidal gold was used to detect the primary antibodies.

Assay to measure membrane-associated VPS26 and VPS35

Cells grown in tissue culture dishes (either 90 mm or 60 mm) were washed with PBS and allowed to drain on ice. After removal of the remaining PBS, the cells were snap frozen using liquid nitrogen and then thawed on the bench. Either 1 ml or 0.5 ml (for 90 mm or 60 mm dishes, respectively) of buffer (0.1 M Mes-NaOH pH 6.5, 1 mM magnesium acetate, 0.5 mM EGTA, 200 μM sodium orthovanadate and 0.2 M sucrose) was added to each dish and the cells were scraped off and transferred into a 1.5 ml tube on ice. The cells were then centrifuged at 10,000 × ***g*** for 5 minutes and the supernatant (which contained cytosolic proteins) was transferred to a fresh tube. The pellet was then solubilised in 1 ml or 0.5 ml (for 90 mm or 60 mm dishes, respectively) of lysis buffer (50 mM Tris-HCl, pH 7.4, 150 mM NaCl, 1 mM EDTA, 1% Triton X-100, 0.1% SDS) before centrifugation at 10,000 × ***g*** for 5 minutes. The supernatant from the second spin now contained membrane and membrane-associated proteins. Equal volumes of the pellet (membrane) and supernatant (cytosol) fractions were subjected to SDS-PAGE and then transferred to nitrocellulose for western blotting.

Native immunoprecipitation

Native immunoprecipitations were performed essentially the same as previously described (Seaman, 2007; Gokool et al., 2007). The native immunoprecipitation in which TBC1D5 was identified as a retromer-interacting protein was performed in an identical fashion, except that the lysis buffer used was PBS with 1% Triton X-100.

Mass spectrometry

Proteins were identified by standard techniques of mass fingerprinting and fragmentation of peptide mixtures generated by in-gel trypsin digestion. Briefly, gel bands were excised and digested with trypsin according to a published method (Shevchenko et al., 1996). Samples of tryptic peptide mixtures were mixed with α-cyano-4-hydroxy-transcinnamic acid matrix and analysed with an ABI 4700 Proteomics Analyser with TOFTOF optics (Applied Biosystems). For peptide mass fingerprints, mass calibration was performed with features internal to the spectrum, specifically the matrix-related ion peak at 1060.048 m/z and the trypsin autolysis peaks at 2163.057 m/z and 2273.160 m/z. For peptide fragment specta, an external mass calibration was generated from the 2163.057 m/z trypsin autolysis peak, using the y10, y14 and y16 fragmentions, and applied to sample spectra. Interpretation was performed by the Mascot sequence database search engine (http://www.matrixscience.com) configured with the gel-derived variable modifications propionamide cysteine and methionine sulfoxide. The NCBI non-redundant (nr) database version as of 11/11/2005 (3023944 sequences; 1040428944 residues) was used as a data set.

We wish to thank colleagues Scottie Robinson, Paul Luzio, David Owen and Folma Buss for many helpful discussions. This work was funded by the Medical Research Council. Deposited in PMC for release after 6 months.

References

Arighi, C. N., Hartnell, L. M., Aguilar, R. C., Haft, C. R. and Bonifacino, J. S. (2004). Role of the mammalian retromer in sorting of the cation-independent mannose 6-phosphate receptor. *J. Cell Biol.* **165**, 123-133.

Bache, K. G., Raiborg, C., Mehlum, A. and Stenmark, H. (2003). STAM and Hrs are subunits of a multivalent ubiquitin-binding complex on early endosomes. *J. Biol. Chem.* **278**, 12513-12521.

Barlowe, C., Orci, L., Yeung, T., Hosobuchi, M., Hamamoto, S., Salama, N., Rexach, M. F., Ravazzola, M., Amherdt, M. and Schekman, R. (1994). COPII: a membrane coat formed by Sec proteins that drive vesicle budding from the endoplasmic reticulum. *Cell* **77**, 895-907.

Béthune, J., Wieland, F. and Moelleken, J. (2006). COPI-mediated transport. *J. Membr. Biol*. **211**, 65-79.

Bonifacino, J. S. and Traub, L. M. (2003). Signals for sorting of transmembrane proteins to endosomes and lysosomes. *Annu. Rev. Biochem*. **72**, 395-447.

Bonifacino, J. S. and Rojas, R. (2006). Retrograde transport from endosomes to the trans-Golgi network. *Nat. Rev. Mol. Cell. Biol*. **7**, 568-579.

Bucci, C., Parton, R. G., Mather, I. H., Stunnenberg, H., Simons, K., Hoflack, B. and Zerial, M. (1992). The small GTPase rab5 functions as a regulatory factor in the early endocytic pathway. *Cell* **70**, 715-728.

Bucci, C., Thomsen, P., Nicoziani, P., McCarthy, J. and van Deurs, B. (2000). Rab7: a key to lysosome biogenesis. *Mol. Biol. Cell* **11**, 467-480.

Burda, P., Padilla, S. M., Sarkar, S. and Emr, S. D. (2002). Retromer function in endosome-to-Golgi retrograde transport is regulated by the yeast Vps34 PtdIns 3-kinase. *J. Cell Sci.* **115**, 3889-3900.

Carlton, J., Bujny, M., Peter, B. J., Oorschot, V. M., Rutherford, A., Mellor, H., Klumperman, J., McMahon, H. T. and Cullen, P. J. (2004). Sorting nexin-1 mediates tubular endosome-to-TGN transport through coincidence sensing of high- curvature membranes and 3-phosphoinositides. *Curr. Biol*. **14**, 1791-1800.

Collins, B. M., Skinner, C. F., Watson, P. J., Seaman, M. N. and Owen, D. J. (2005). Vps29 has a phosphoesterase fold that acts as a protein interaction scaffold for retromer assembly. *Nat. Struct. Mol. Biol*. **12**, 594-602.

Collins, B. M., Norwood, S. J., Kerr, M. C., Mahony, D., Seaman, M. N., Teasdale, R. D. and Owen, D. J. (2008). Structure of Vps26B and mapping of its interaction with the retromer protein complex. *Traffic* **9**, 366-379.

Cullen, P. J. (2008). Endosomal sorting and signalling: an emerging role for sorting nexins. *Nat. Rev. Mol. Cell. Biol*. **9**, 574-582.

Driskell, O. J., Mironov, A., Allan, V. J. and Woodman, P. G. (2007). Dynein is required for receptor sorting and the morphogenesis of early endosomes. *Nat. Cell Biol*. **9**, 113-120.

Eaton, S. (2008). Retromer retrieves wntless. *Dev. Cell* **14**, 4-6.

Eichner-Techau, M., Valdez-Taubas, J., Popoff, J. F., Francis, R., Seaman, M. and Blackwell, J. M. (2007). Evolution of differences in transport function in Slc11a family members. *J. Biol. Chem.* **282**, 35646-35656.

Eugster, A., Frigerio, G., Dale, M. and Duden, R. (2000). COP I domains required for coatomer integrity, and novel interactions with ARF and ARF-GAP. *EMBO J*. **19**, 3905-3917.

Fukuda, M. (2008). Regulation of secretory vesicle traffic by Rab small GTPases. *Cell Mol. Life Sci*. **65**, 2801-2813.

Giot, L., Bader, J. S., Brouwer, C., Chaudhuri, A., Kuang, B., Li, Y., Hao, Y. L., Ooi, C. E., Godwin, B., Vitols, E. et al. (2003). A protein interaction map of Drosophila melanogaster. *Science* **302**, 1727-1736.

Gokool, S., Tattersall, D. and Seaman, M. N. (2007). EHD1 interacts with retromer to stabilize SNX1 tubules and facilitate endosome-to-Golgi retrieval. *Traffic* **8**, 1873-1886.

Goody, R. S., Rak, A. and Alexandrov, K. (2005). The structural and mechanistic basis for recycling of Rab proteins between membrane compartments. *Cell Mol. Life Sci*. **62**, 1657-1670.

Haft, C. R., de la Luz Sierra, M., Bafford, R., Lesniak, M. A., Barr, V. A. and Taylor, S. I. (2000). Human orthologs of yeast vacuolar protein sorting proteins Vps26, 29, and **35**, assembly into multimeric complexes. *Mol. Biol. Cell* **11**, 4105-4116.

Hierro, A., Rojas, A. L., Rojas, R., Murthy, N., Effantin, G., Kajava, A. V., Steven, A. C., Bonifacino, J. S. and Hurley, J. H. (2007). Functional architecture of the retromer cargo-recognition complex. *Nature* **449**, 1063-1067.

Houlden, H., King, R. H., Muddle, J. R., Warner, T. T., Reilly, M. M., Orrell, R. W. and Ginsberg, L. (2004). A novel RAB7 mutation associated with ulcero-mutilating neuropathy. *Ann. Neurol*. **56**, 586-590.

Johansson, M., Rocha, N., Zwart, W., Jordens, I., Janssen, L., Kuijl, C., Olkkonen, V. M. and Neefjes, J. (2007). Activation of endosomal dynein motors by stepwise assembly of Rab7-RILP p150Glued, ORP1L, and the receptor betalll spectrin. *J. Cell Biol*. **176**, 459-471.

Lam-Yuk-Tseung, S. and Gros, P. (2006). Distinct targeting and recycling properties of two isoforms of the iron transporter DMT1 (NRAMP2, Slc11A2). *Biochemistry* **45**, 2294-2301.

Letourneur, F., Gaynor, E. C., Hennecke, S., Démollière, C., Duden, R., Emr, S. D., Riezman, H. and Cosson, P. (1994). Coatomer is essential for retrieval of dilysine-tagged proteins to the endoplasmic reticulum. *Cell* **79**, 1199-1207.

Mancias, J. D. and Goldberg, J. (2005). Exiting the endoplasmic reticulum. *Traffic* **6**, 278-285.

McLauchlan, H., Newell, J., Morrice, N., Osborne, A., West, M. and Smythe, E. (1998). A novel role for Rab5-GDI in ligand sequestration into clathrin-coated pits. *Curr. Biol*. **8**, 34-45.

Meggouh, F., Bienfait, H. M., Weterman, M. A., de Visser, M. and Baas, F. (2006). Charcot-Marie-Tooth disease due to a *de novo* mutation of the RAB7 gene. *Neurology*. **67**, 1476-1478.

Muhammad, A., Flores, I., Zhang, H., Yu, R., Staniszewski, A., Planel, E., Herman, M., Ho, L., Kreber, R., Honig, L. S. et al. (2008). Retromer deficiency observed in Alzheimer's disease causes hippocampal dysfunction, neurodegeneration, and Abeta accumulation. *Proc. Natl. Acad. Sci. USA* **105**, 7327-7332.

Mukhopadhyay, A., Pan, X., Lambright, D. G. and Tissenbaum, H. A. (2007). An endocytic pathway as a target of tubby for regulation of fat storage. *EMBO Rep*. **8**, 931-938.

Nakada-Tsukui, K., Saito-Nakano, Y., Ali, V. and Nozaki, T. (2005). A retromerlike complex is a novel Rab7 effector that is involved in the transport of the virulence factor cysteine protease in the enteric protozoan parasite Entamoeba histolytica. *Mol. Biol. Cell* **16**, 5294-5303.

Nothwehr, S. F., Ha, S. A. and Bruinsma, P. (2000). Sorting of yeast membrane proteins into an endosome-to-Golgi pathway involves direct interaction of their cytosolic domains with Vps35p. *J. Cell Biol*. **151**, 297-310.

Orci, L., Palmer, D. J., Amherdt, M. and Rothman, J. E. (1993). Coated vesicle assembly in the Golgi requires only coatomer and ARF proteins from the cytosol. *Nature* **364**, 732-734.

Palmer, D. J., Helms, J. B., Beckers, C. J., Orci, L. and Rothman, J. E. (1993). Binding of coatomer to Golgi membranes requires ADP-ribosylation factor. *J. Biol. Chem*. **268**, 12083-12089.

Pan, X., Eathiraj, S., Munson, M. and Lambright, D. G. (2006). TBC-domain GAPs for Rab GTPases accelerate GTP hydrolysis by a dual-finger mechanism. *Nature* **442**, 303-306.

Popoff, V., Mardones, G. A., Tenza, D., Rojas, R., Lamaze, C., Bonifacino, J. S., Raposo, G. and Johannes, L. (2007). The retromer complex and clathrin define an early endosomal retrograde exit site. *J. Cell Sci.* **120**, 2022-2031.

Reddy, J. V. and Seaman, M. N. (2001). Vps26p, a component of retromer, directs the interactions of Vps35p in endosome-to-Golgi retrieval. *Mol. Biol. Cell* **12**, 3242-3256.

Reddy, J. V., Burguete, A. S., Sridevi, K., Ganley, I. G., Nottingham, R. M. and Pfeffer, S. R. (2006). A functional role for the GCC185 golgin in mannose 6-phosphate receptor recycling. *Mol. Biol. Cell* **17**, 4353-4363.

Riederer, M. A., Soldati, T., Shapiro, A. D., Lin, J. and Pfeffer, S. R. (1994). Lysosome biogenesis requires Rab9 function and receptor recycling from endosomes to the trans-Golgi network. *J. Cell Biol*. **125**, 573-582.

Rink, J., Ghigo, E., Kalaidzidis, Y. and Zerial, M. (2005). Rab conversion as a mechanism of progression from early to late endosomes. *Cell* **122**, 735-749.

Rojas, R., Kametaka, S., Haft, C. R. and Bonifacino, J. S. (2007). Interchangeable but essential functions of SNX1 and SNX2 in the association of retromer with endosomes and the trafficking of mannose 6-phosphate receptors. *Mol. Cell. Biol*. **27**, 1112-1124.

Rojas, R., van Vlijmen, T., Mardones, G. A., Prabhu, Y., Rojas, A. L., Mohammed, S., Heck, A. J., Raposo, G., van der Sluijs, P. and Bonifacino, J. S. (2008). Regulation of retromer recruitment to endosomes by sequential action of Rab5 and Rab7. *J. Cell Biol*. **183**, 513-526.

Seaman, M. N. (2004). Cargo-selective endosomal sorting for retrieval to the Golgi requires retromer. *J. Cell Biol*. **165**, 111-122.

Seaman, M. N. (2007). Identification of a novel conserved sorting motif required for retromer-mediated endosome-to-TGN retrieval. *J. Cell Sci*. **120**, 2378-2389.

Seaman, M. N. (2005). Recycle your receptors with retromer. *Trends Cell Biol*. **15**, 68-75.

Seaman, M. N. (2008). Endosome protein sorting: motifs and machinery. *Cell Mol. Life Sci*. **65**, 2842-2858.

Semerdjieva, S., Shortt, B., Maxwell, E., Singh, S., Fonarev, P., Hansen, J., Schiavo, G., Grant, B. D. and Smythe, E. (2008). Coordinated regulation of AP2 uncoating from clathrin-coated vesicles by rab5 and hRME-6. *J. Cell Biol*. **183**, 499-511.

Shevchenko, A., Wilm, M., Vorm, O. and Mann, M. (1996). Mass spectrometric sequencing of proteins from silver-stained polyacrylamide gels. *Anal. Chem*. **68**, 850-858.

Small, S. A., Kent, K., Pierce, A., Leung, C., Kang, M. S., Okada, H., Honig, L., Vonsattel, J. P. and Kim, T. W. (2005). Model-guided microarray implicates the retromer complex in Alzheimer's disease. *Ann. Neurol*. **58**, 909-919.

Spang, A. (2008). The life cycle of a transport vesicle. *Cell Mol. Life Sci*. **65**, 2781-2789.

Stamnes, M. A. and Rothman, J. E. (1993). The binding of AP-1 clathrin adaptor particles to Golgi membranes requires ADP-ribosylation factor, a small GTP-binding protein. *Cell* **73**, 999-1005.

Stein, M. P., Feng, Y., Cooper, K. L., Welford, A. M. and Wandinger-Ness, A. (2003). Human VPS34 and p150 are Rab7 interacting partners. *Traffic* **4**, 754-771.

Szafer, E., Rotman, M. and Cassel, D. (2001). Regulation of GTP hydrolysis on ADP-ribosylation factor-1 at the Golgi membrane. *J. Biol. Chem*. **276**, 47834-47839.

Verhoeven, K., De Jonghe, P., Coen, K., Verpoorten, N., Auer-Grumbach, M., Kwon, J. M., FitzPatrick, D., Schmedding, E., De Vriendt, E., Jacobs, A. et al. (2003). Mutations in the small GTP-ase late endosomal protein RAB7 cause Charcot-Marie-Tooth type 2B neuropathy. *Am. J. Hum. Genet*. **72**, 722-727.

Yoshihisa, T., Barlowe, C. and Schekman, R. (1993). Requirement for a GTPase-activating protein in vesicle budding from the endoplasmic reticulum. *Science* **259**, 1466-1468.

Zerial, M. and McBride, H. (2001). Rab proteins as membrane organizers. *Nat. Rev. Mol. Cell Biol*. **2**, 107-117.

5 nm = anti-VPS26, 10 nm = anti-GFP.

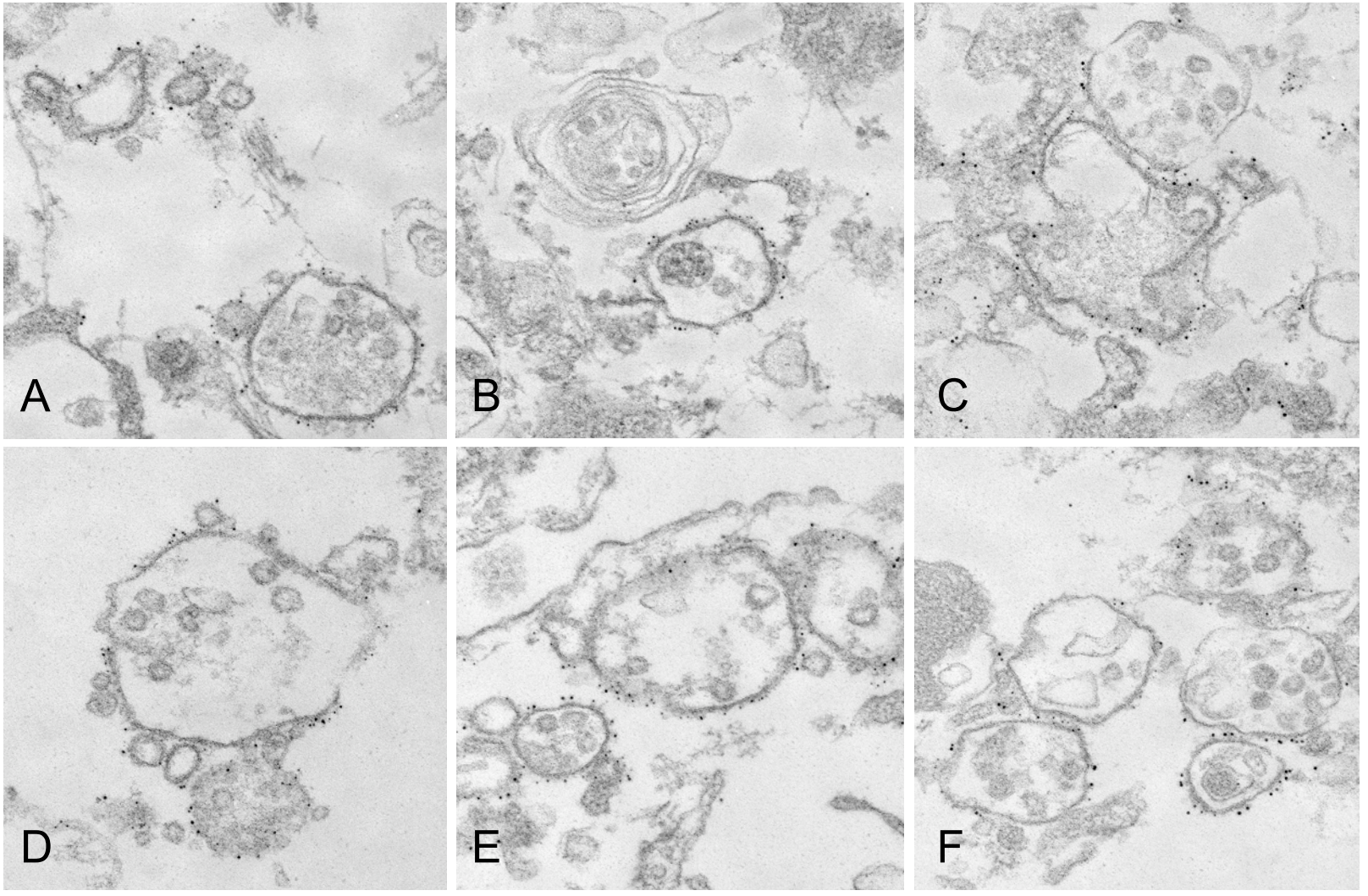

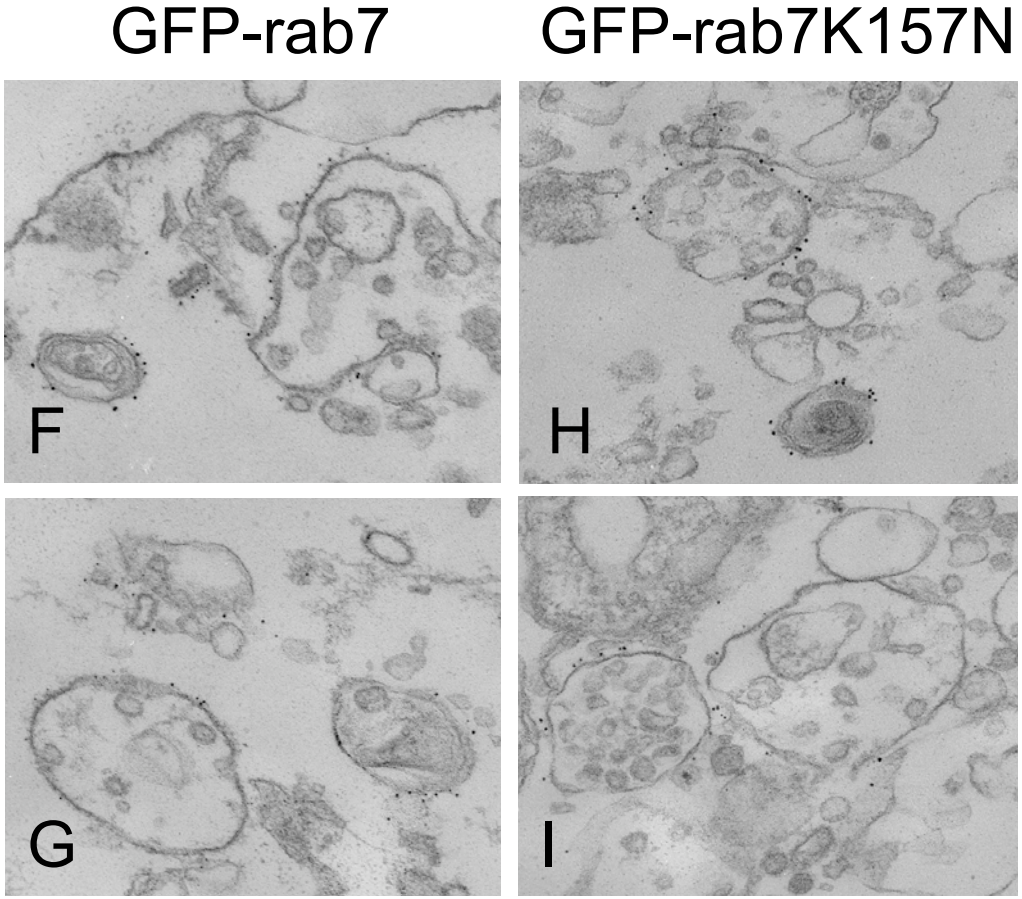
GFP-rab7
GFP-rab7K157N
F
H
G
I

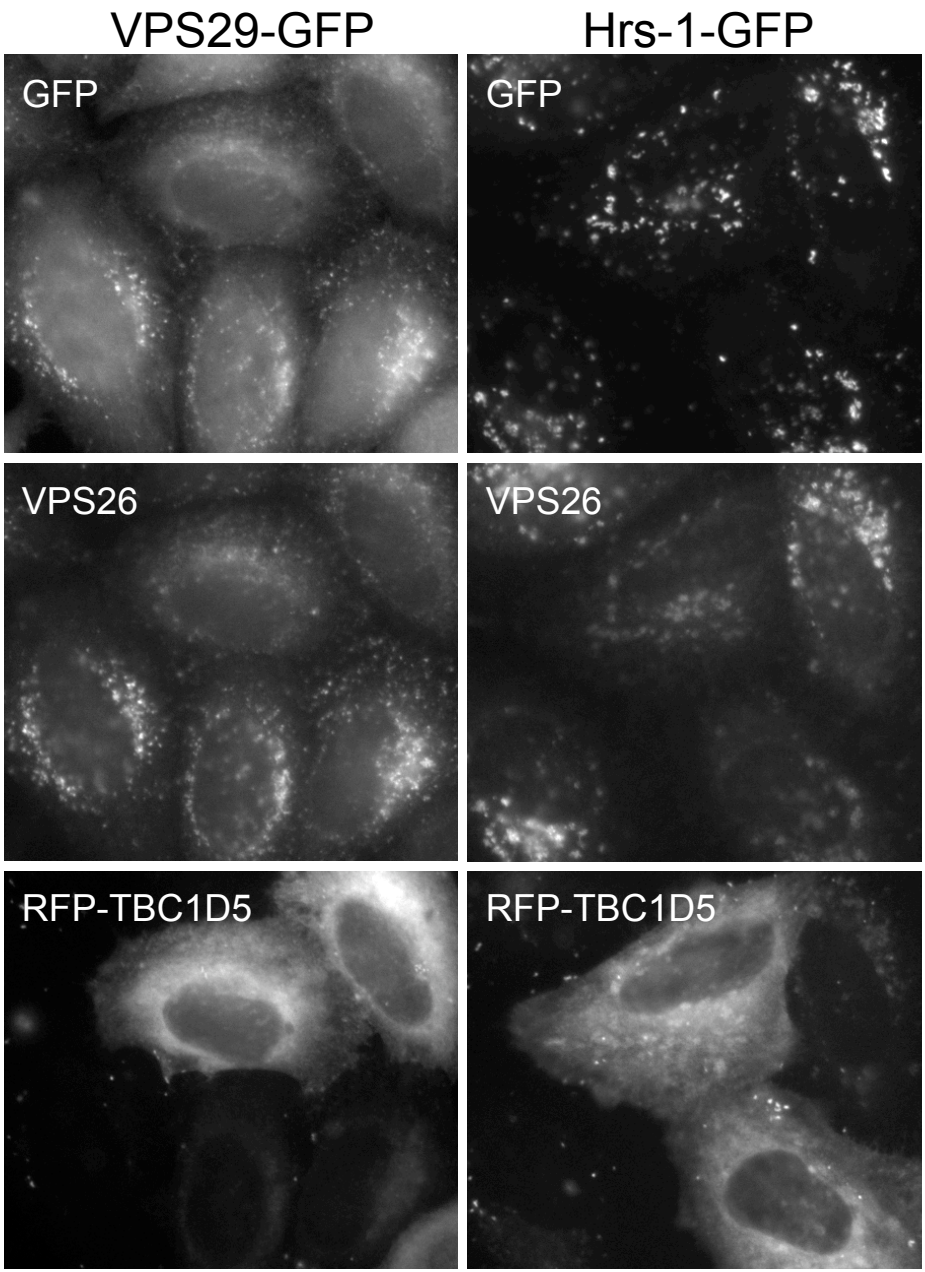
VPS29-GFP
Hrs-1-GFP
GFP
GFP
VPS26
VPS26
RFP-TBC1D5
RFP-TBC1D5

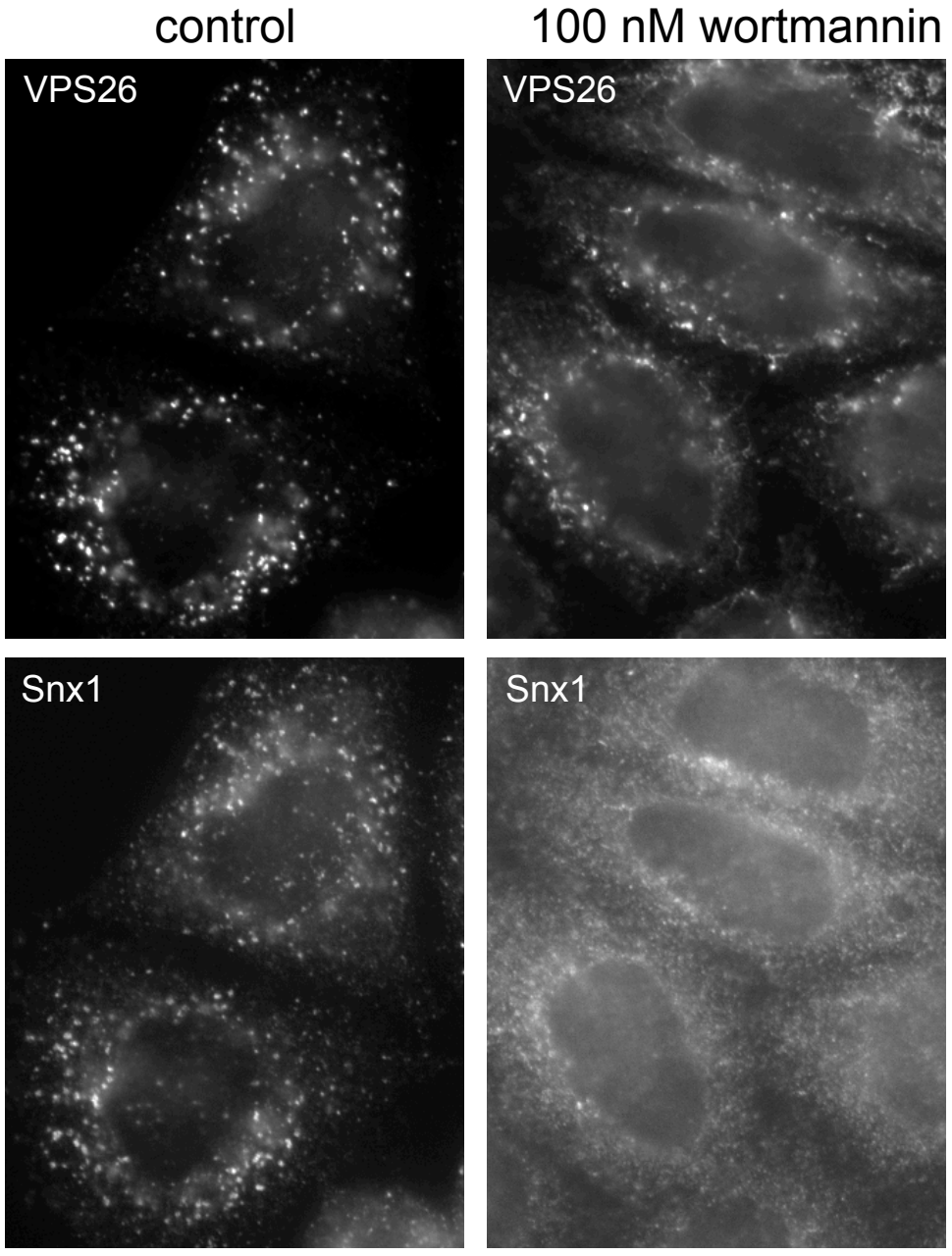
control
100 nM wortmannin
VPS26
VPS26
Snx1
Snx1

Table S1. Mass spectrometry analysis of GFP-rab native IPs								
Candidate (NCBInr accn#)	MALDI-MS data			Supporting tandem MS data				
	Peptide matches[A]	Sequence coverage %	Mascot PMF Score[B]	Peptide Ion mass/charge ratio [MH+]		Amino Acid Residues	Sequence	Mascot Individual Ions Score[B]
				Observed	Expected from Database Record			
1. RAB9, member RAS oncogene family (gil9790227)	7/27	43	154/76	2447.108	2447.122	48 - 68	K.DLEVDGHFVTMQIWDTAGQER.F	119/46
				1479.846	1479.700	157 - 170	K.DSTNVAAAFEEAVR.R	20/46
				1635.922	1635.801	157 - 171	K.DSTNVAAAFEEAVRR.I	26/46
				1662.965	1662.849	179 - 192	R.SEHLIQTDTVNLHR.K	112/46
2. GDP dissociation inhibitor 2 (gil30582575)	24/50	56	154/76	1402.741	1402.707	56 - 68	R.FKIPGSPPESMGR.G	15/46
				1125.627	1125.590	90 - 98	K.MLLYTEVTR.Y	16/46
				1916.838	1916.826	194 - 208	R.TDDYLDQP(PamC)YETINR.I	63/46
				2141.113	2141.099	222 - 240	K.SPYLYPLYGLGELPQGFAR.L	43/46
				2213.085	2213.065	310 - 328	K.NTNDANS(PamC)QIIIPQNQVNR.K	27/46
				1778.022	1777.999	365 - 379	K.EIRPALELLEPIEQK.F	21/46
				1365.724	1365.694	391 - 402	K.DLGTESQIFISR.T	74/46
3. VPS26A (gil3342000)	n/a	n/a	n/a	1313.730	1313.699	94 - 105	K.ELALPGELTQSR.S	9/46
				923.569	923.564	195 - 201	K.IYFLLVR.I	2/46
				1624.866	1624.814	272 - 284	R.YFLNLVLVDEEDR.S	10/46
				1085.624	1085.603	289 - 296	K.QQEIILWR.K	10/46
4. GDP dissociation inhibitor 2 (gil30582575)	25/47	64	175/76	1402.755	1402.707	56 - 68	R.FKIPGSPPESMGR.G	18/46
				1916.861	1916.826	194 - 208	R.TDDYLDQP(PamC)YETINR.I	38/46
				2213.075	2213.065	310 - 328	K.NTNDANS(PamC)QIIIPQNQVNR.K	16/46
				1778.052	1777.999	365 - 379	K.EIRPALELLEPIEQK.F	21/46
				1365.732	1365.694	391 - 402	K.DLGTESQIFISR.T	40/46
5. RAB7, member RAS oncogene family (gil56269740)	17/35	76	152/76	1647.854	1647.809	56 - 69	R.LVTMQIWDTAGQER.F	83/46
				1187.641	1187.613	70 - 79	R.FQSLGVAFYR.G	62/46

				1934.001	1933.969	98 - 113	K.TLDSWRDEFLIQASPR.D	21/46
				1175.621	1175.598	104 - 113	R.DEFLIQASPR.D	86/46
				1475.777	1475.746	114 - 126	R.DPENFPFVVLGNK.I	52/46
				1589.865	1589.821	158 - 171	K.EAINVEQAFQTIAR.N	110/46
6. vacuolar sorting protein 35 (gil9622850)	14/39	21	54/76	1762.894	1762.853	500 - 514	R.SEDPDQQYLILNTAR.K	28/46
7. choroideremia (Rab escort protein 1) (gil9966761)	n/a	n/a	n/a	2474.214	2474.234	466 - 488	K.TDSDQQISILTVPAEEPGTFAVR.V	26/46
8. GDP dissociation inhibitor 2 (gil30582575)	30/48	65	206/76	1402.726	1402.707	56 - 68	R.FKIPGSPPESMGR.G	46/46
				1312.707	1312.694	69 - 79	R.GRDWNVDLIPK.F	35/46
				1125.608	1125.590	90 - 98	K.MLLYTEVTR.Y	16/46
				1344.671	1344.676	143 - 153	K.FLVYVANFDEK.D	59/46
				1916.834	1916.826	194 - 208	R.TDDYLDQP(PamC)YETINR.I	80/46
				938.501	938.494	211 - 218	K.LYSESLAR.Y	21/46
				2141.113	2140.099	222 - 240	K.SPYLYPLYGLGELPQGFAR.L	107/46
				2213.080	2213.065	310 - 328	K.NTNDANS(PamC)QIIIPQNQVNR.K	47/46
				1778.009	1777.999	365 - 379	K.EIRPALELLEPIEQK.F	30/46
				1365.710	1365.694	391 - 402	K.DLGTESQIFISR.T	104/46
				1606.692	1606.680	424 - 436	R.MTGSEFDFEEMKR.K	59/46
9. Rab5c protein (gil20988213)	13/47	78	79/76	1351.662	1351.620	72 - 82	K.FEIWDTAGQER.Y	77/46
				1300.644	1300.607	83 - 92	R.YHSLAPMYYR.G	57/46
				2026.037	2026.017	93 - 111	R.GAQAAIVVYDITNTDTFAR.A	142/46
				2678.155	2678.222	143 - 166	R.AVEFQEAQAYADDNSLLFMETSAK.T	76/46
				1552.814	1552.779	167 - 180	K.TAMNVNEIFMAIAK.K	72/46
				1181.584	1181.558	185 - 196	K.NEPQNAAGAPGR.T	68/46
10. GDP dissociation inhibitor 1 (gil54696630)	17/31	48	123/76	1460.784	1460.713	56 - 68	R.FQLLEGPPESMGR.G	34/46
				1125.622	1125.590	90 - 98	K.MLLYTEVTR.Y	24/46
				1468.727	1468.666	157 - 169	K.TFEGVDPQTTSMR.D	18/46
				1852.885	1852.831	194 - 208	R.TDDYLDQP(PamC)LETVNR.I	81/46
				2213.082	2213.065	310 - 328	K.NTNDANS(PamC)QIIIPQNQVNR.K	18/46
				1361.633	1361.5791	424 - 435	R.MAGTAFDFENMK.R	66/46

Candidate (NCBInr accn#)	MALDI-MS data			Supporting tandem MS data				
	Peptide matches[A]	Sequence coverage %	Mascot PMF Score[B]	Peptide Ion mass/charge ratio [MH+]		Amino Acid Residues	Sequence	Mascot Individual Ions Score[B]
				Observed	Expected from Database Record			
11. VPS26A (gil3342000)	6/20	21	59/77	nd[C]	nd	nd	nd	nd
12. RAB7, member RAS oncogene family (gil56269740)	6/16	33	72/76	1187.559	1187.613	70 - 79	R.FQSLGVAFYR.G	48/46
				1933.855	1933.969	98 - 113	K.TLDSWRDEFLIQASPR.D	21/46
				1175.550	1175.598	104 - 113	R.DEFLIQASPR.D	36/46
				1589.739	1589.821	158 - 171	K.EAINVEQAFQTIAR.N	82/46
				1632.753	1632.842	56 - 69	R.LVTMQIWDTAG[**L**]ER.F	bi[D]
13. RAB7, member RAS oncogene family (gil56269740)	12/30	63	128/76	1647.732	1647.809	56 - 69	R.LVTMQIWDTAG[**Q**]ER.F	55/46
				1663.716	1663.804	56 - 69	R.LVT(MetOx)QIWDTAG[**Q**]ER.F	17/46
				1187.554	1187.613	70 - 79	R.FQSLGVAFYR.G	68/46
				1933.883	1933.969	98 - 113	K.TLDSWRDEFLIQASPR.D	26/46
				1175.544	1175.598	104 - 113	R.DEFLIQASPR.D	38/46
				1589.742	1589.821	158 - 171	K.EAINVEQAFQTIAR.N	99/46
14. GDP dissociation inhibitor 1 (gil54696630)	22/30	48	256/76	1027.554	1027.539	104 - 112	K.VVEGSFVYK.G	19/46
				1654.747	1654.804	143 - 156	K.FLVFVANFDENDPK.T	64/46
				1852.784	1852.831	194 - 208	R.TDDYLDQP(PamC)LETVNR.I	48/46
				2141.095	2141.099	222 - 240	K.SPYLYPLYGLGELPQGFAR.L	27/46
				1722.842	1722.909	366 - 380	K.EVEPALELLEPIDQK.F	39/46
15. vacuolar sorting protein 35 (gil9622850)	9/19	14	73/76	nd[C]	nd	nd	nd	nd
16. vacuolar sorting protein 35 (gil9622850)	11/22	15	89/76	nd[C]	nd	nd	nd	nd

Table S2. Identification of the retromer interacting protein, TBC1D5								
Candidate (NCBInr accn#)	MALDI-MS data			Supporting tandem MS data				
	Peptide matches[A]	Sequence coverage %	Mascot PMF Score[B]	Peptide Ion mass/charge ratio [MH+]		Amino Acid Residues	Sequence	Mascot Individual Ions Score[B]
				Observed	Expected from Database Record			
1.TBC1D5 (gil15341918)	38/94	44	237/76	2139.068	2139.080	57 - 73	R.KEWEELFVNNNYLATIR.Q	23/45
				2010.976	2010.985	58 - 73	K.EWEELFVNNNYLATIR.Q	105/45
				1800.826	1800.830	170 - 183	R.TFPEMQFFQQENVR.K	89/45
				1272.727	1272.724	323 - 333	R.LEIAPQIYGLR.W	43/45
				1106.593	1106.588	457 - 466	K.VSNSLINFGR.K	78/45
				2101.999	2102.005	499 - 516	R.TSAEAPSHHLQQQQQQQR.L	102/45
				1147.583	1147.578	729 - 739	R.GSFSGQAQPLR.T	56/45
2. Vacuolar protein sorting 35 (gil17999541)	54/105	59	338/76	1127.576	1127.555	45 - 54	K.HASNMLGELR.T	70/45
				1243.682	1243.659	227 - 237	R.LSQLEGVNVER.Y	62/45
				1852.006	1851.989	324 - 339	K.LFDIFSQQVATVIQSR.Q	64/45
				1886.841	1886.842	420 - 433	K.HFHPLFEYFDYESR.K	24/45
				1762.871	1762.853	500 - 514	R.SEDPDQQYLILNTAR.K	103/45
				943.467	943.442	516 - 524	K.HFGAGGNQR.I	58/45
				1616.946	1616.930	623 - 637	K.AQLAAITLIIGTFER.M	76/45
				2244.101	2244.092	750 - 768	K.IREDLPNLESSEETEQINK.H	55/45
				1303.675	1303.659	769 - 778	K.HFHNTLEHLR.L	76/45
3. VPS26B (gil30023568)	17/45	38	85/76	923.592	923.564	193 - 199	K.IYFLLVR.I	15/45
				1668.864	1668.841	270 - 282	R.YYLNLVLIDEEER.R	58/45
				1057.599	1057.572	287 - 294	K.QQEVVLWR.K	33/45
				1195.610	1195.588	314 - 324	R.FEGTTSLGEVR.T	65/45
4. VPS26A (gil3342000)	24/71	66	109/76	1313.816	1313.699	94 - 105	K.ELALPGELTQSR.S	58/45

				2688.487	2688.2213	106 - 127	R.SYDFEF(MetOx)QVEKPYESYIGANVR.L	44/45
				2332.388	2332.175	146 - 165	K.EYDLIVHQLATYPDVNNSIK.M	64/45
				923.648	923.564	195 - 201	K.IYFLLVR.I	15/45
				1891.116	1890.956	233 - 249	K.YEI(MetOx)DGAPVKGESIPIR.L	33/45
				1624.965	1624.814	272 - 284	R.YFLNLVLVDEEDR.S	80/45
				1085.702	1085.603	289 - 296	K.QQEIILWR.K	56/45
5. Hrs (gil9506795)	31/66	39	220/76	1601.908	1601.888	108 - 120	K.ILYLIQAWAHAFR.N	41/45
				2839.483	2839.476	227 - 252	K.AASTTELPPEYLTSPLSQQSQLPPKR.D	93/45
				3663.822	3663.795	292 - 328	K.SEPAPLASSAPPAGSLYSSPVNSSAPLAEDIDPELAR.Y	47/45
				1319.722	1319.699	410 - 421	K.ALQNAVSTFVNR.M	92/45
				3110.649	3110.641	431 - 458	R.SITNDSAVLSLFQSINSTHPQLLELLNR.L	44/45
				1192.647	1192.625	520 - 528	K.KQEYLEVQR.Q	36/45
				1064.553	1064.530	521 - 528	K.QEYLEVQR.Q	31/45
6. signal transducing adaptor molecule (gil4507249).	n/a	n/a	n/a	2786.561	2786.363	189 - 213	R.QQSTTLSTLYPSTSSLLTNHQHEGR.K	24/45

[A]number of mass matches/total number of masses searched
[B]Scores are shown with associated threshold score for p(match)<0.05